

Arbitrarily high-order energy-preserving schemes for the Zakharov-Rubenchik equation

Gengen Zhang^a, Chaolong Jiang^{b,c,*}, Hao Huang^b

^a*School of Mathematics and Statistics, Yunnan University, Kunming 650504, China*

^b*School of Statistics and Mathematics, Yunnan University of Finance and Economics, Kunming 650221, China*

^c*Department of Mathematics, College of Liberal Arts and Science, National University of Defense Technology, Changsha 410073, China*

Abstract

In this paper, we present a high-order energy-preserving scheme for solving Zakharov-Rubenchik equation. The main idea of the method is first to reformulate the original system into an equivalent one by introducing a quadratic auxiliary variable, and the symplectic Runge-Kutta method, together with the Fourier pseudo-spectral method is then employed to compute the solution of the reformulated system. The main benefit of the proposed method is that it can conserve the three invariants of the original system and achieves arbitrarily high-order accurate in time. In addition, an efficient fixed-point iteration is proposed to solve the resulting nonlinear equations of the proposed schemes. Several experiments are provided to validate the theoretical results.

Keywords: Zakharov-Rubenchik equation; energy-preserving; Runge-Kutta method; quadratic auxiliary variable approach; Fourier pseudo-spectral method.

1. Introduction

The Zakhrov-Rubenchik (ZR) equation is applied extensively to describe the interaction and the dynamics of spectrally narrow high-frequency waves with low-frequency (acoustic) waves [34]. In this paper, we consider the following ZR equation

$$\begin{cases} i\partial_t B(x, t) + \omega \partial_{xx} B(x, t) - \kappa(u(x, t) - \frac{1}{2}\nu\rho(x, t) + q|B(x, t)|^2)B(x, t) = 0, \\ \partial_t \rho(x, t) + \partial_x(u(x, t) - \nu\rho(x, t)) = -\kappa \partial_x(|B(x, t)|^2), \\ \partial_t u(x, t) + \partial_x(\beta\rho(x, t) - \nu u(x, t)) = \frac{1}{2}\kappa\nu \partial_x(|B(x, t)|^2), \end{cases} \quad x \in \mathbb{R}, \quad t > 0, \quad (1.1)$$

with the initial conditions

$$B(x, 0) = B_0(x), \quad \rho(x, 0) = \rho_0(x), \quad u(x, 0) = u_0(x), \quad x \in \mathbb{R}, \quad (1.2)$$

where the complex-valued function $B := B(x, t)$ denotes the magnetic field generated by the plasma, $\rho := \rho(x, t)$ and $u := u(x, t)$ are the real-valued functions, which represent the density of mass and the fluid speed, respectively. Moreover, ω , κ , ν , β and q are given real constants where ω and κ denote the frequency and the wave number, respectively, ν and β are dimensionless parameters, and q satisfies

$$q = \kappa + \frac{\nu(\kappa\nu - 1)}{4(\beta - \nu^2)}.$$

The ZR equation (1.1) conserves the following three invariants

- Mass

$$\mathcal{M}(t) = \int_{\mathbb{R}} |B|^2 dx \equiv \mathcal{M}(0), \quad t \geq 0, \quad (1.3)$$

*Corresponding author

Email addresses: zhanggen036@163.com (Gengen Zhang), Chaolong\$_{j}\$jiang@126.com (Chaolong Jiang), 793050920@qq.com (Hao Huang)

- Hamiltonian energy

$$\mathcal{H}(t) = \int_{\mathbb{R}} \left(-\omega|B_x|^2 - \kappa \left(u - \frac{\nu}{2}\rho + \frac{q}{2}|B|^2 \right) |B|^2 - \frac{\beta}{2}\rho^2 - \frac{1}{2}u^2 + \nu u \rho \right) dx, \quad t \geq 0, \quad (1.4)$$

- Two linear invariants

$$\mathcal{I}_1(t) = \int_{\mathbb{R}} \rho \, dx \equiv \mathcal{I}_1(0), \quad \mathcal{I}_2(t) = \int_{\mathbb{R}} u \, dx \equiv \mathcal{I}_2(0), \quad t \geq 0. \quad (1.5)$$

Extensive theoretical studies have been carried out for the equation (1.1) in the literature. For the well-posedness and existence of the ZR equation (1.1), we refer to [19, 22, 24, 26] and references therein. In particular, Oliveira [22] not only proved local and global well-posedness of the ZR equation (1.1) for initial data in $H_2(\mathbb{R}) \times H_1(\mathbb{R}) \times H_1(\mathbb{R})$, but also studied orbital stability and existence of the solitary wave solutions. For the asymptotic behavior of solutions and the adiabatic limit of the ZR equation (1.1), we refer to [8] and [23], respectively.

A numerical scheme that preserves one or more invariants of the original system is known as an energy-preserving scheme. It is shown in [29, 35] that the non-energy-preserving scheme will produce nonlinear blow-up in the numerical simulation of soliton collisions. Thus, over the last decade, there are some literatures concerning the energy-preserving schemes for the ZR equation (1.1). Zhao et al. [37] proposed a time-splitting Fourier pseudo-spectral (TS-FP) scheme and a Crank-Nicolson finite difference (CN-FD) scheme, respectively. It is proven that the TS-FP scheme can conserve the mass (1.3), and the CN-FD scheme can conserve three invariants (1.4)-(1.5). Later on, the Crank-Nicolson Fourier pseudo-spectral (CN-FP) scheme is investigated and analysed in [38]. Meanwhile, Ji et al. [13] proposed a Crank-Nicolson compact finite difference scheme, which is proven rigorously in mathematics that the scheme is second-order accurate in time and fourth-order accurate in space, respectively. Nevertheless, all of existing energy-preserving schemes are second-order accurate in time. In [9, 14], numerical experiments show that the high-order energy-preserving schemes not only provide much smaller numerical error but also more robust than the second-order accurate schemes. Therefore, it is interesting to design high-order energy-preserving schemes for solving the ZR equation (1.1), which however has not been considered in the literature.

In 1987, Cooper[7] showed that all RK methods conserve linear invariants and an irreducible RK method can preserve all quadratic invariants if and only if their coefficients satisfies the specific algebraic condition. Then, Calvo et al. [4] proved that no RK method can preserve arbitrary polynomial invariants of degree 3 or higher of arbitrary vector fields. Consequently, over the past few decades, there has been an increasing interest in higher-order energy-preserving methods for the general conservative systems. The noticeable ones include high-order averaged vector field methods [16, 20, 27], Hamiltonian Boundary Value Methods (HBVMs) [2, 3], energy-preserving continuous stage Runge-Kutta methods [21, 31], functionally fitted energy-preserving methods [21, 18] and energy-preserving variant of collocation methods [6, 11] etc. However, we note that these mentioned methods can conserve both the Hamiltonian energy and the linear invariant of the original system at most (see [1, 17, 33]). Inspire by the quadratic auxiliary variable (QAV) approach proposed by Gong et al[10], in this paper, we propose a class of high-order numerical schemes which can preserve the three invariants (1.4)-(1.5) of the ZR equation (1.1) exactly.

The rest of this paper is organized as follows. In section 2, based on the idea of the QAV approach, we first reformulate the original ZR equation (1.1) into an equivalent system. In section 3, we present a class of high-order numerical schemes which can conserve the three invariants (1.4)-(1.5) of the ZR equation (1.1). An efficient implementation for solving the nonlinear equations of the proposed scheme is presented in section 4. In section 5, extensive numerical tests and comparisons are carried out to illustrate the performance of the proposed schemes. Section 6 includes the conclusions of this paper.

2. Model reformulation

In this section, the ZR equation (1.1) is first reformulated into an equivalent form, which provides an elegant platform for efficiently developing arbitrarily high-order energy-preserving schemes. Due to the rapid decay of the solution at the far field [19, 22], the ZR equation (1.1) is truncated on a bounded interval $\Omega = [a, b]$ with a periodic boundary condition. In addition, we definite the continuous inner product as $(f, g) = \int_{\Omega} f \bar{g} dx$, for any $f, g \in L^2(\Omega)$ and the L^2 -norm is defined as $\|f\|^2 = (f, f)$.

To be the start, the ZR equation (1.1) can be written as

$$\frac{\partial z}{\partial t} = \mathcal{J} \frac{\delta \mathcal{H}}{\delta \bar{z}}, \quad \mathcal{J} = \begin{pmatrix} i & 0 & 0 \\ 0 & 0 & \partial_x \\ 0 & \partial_x & 0 \end{pmatrix}, \quad (2.1)$$

where $z = (B, \rho, u)^T$, \bar{z} is the complex conjugate of z , and $\frac{\delta \mathcal{H}}{\delta \bar{z}}$ is the variational derivative of the Hamiltonian functional (1.4). Then motivated by [10, 15, 32], we introduce an quadratic auxiliary variable as

$$\phi := \phi(x, t) = |B|^2. \quad (2.2)$$

Then, the Hamiltonian energy (1.4) is reformulated into the following quadratic form

$$\mathcal{E} = \int_{\Omega} \left(-\omega |B_x|^2 - \kappa \left(u - \frac{\nu}{2} \rho + \frac{q}{2} \phi \right) \phi - \frac{\beta}{2} \rho^2 - \frac{1}{2} u^2 + \nu u \rho \right) dx. \quad (2.3)$$

According to the energy variational principle, the equation (2.1) can be written into an equivalent formulation, as follows:

$$\begin{cases} B_t = i(\omega B_{xx} - \kappa(u - \frac{1}{2}\nu\rho + q\phi)B), \\ \rho_t = \partial_x(-u + \nu\rho - \kappa\phi), \\ u_t = \partial_x(-\beta\rho + \nu u + \frac{1}{2}\kappa\nu\phi), \\ \phi_t = 2\text{Re}(B_t \cdot \bar{B}), \quad x \in \Omega, \quad t \geq 0, \end{cases} \quad (2.4)$$

where $\text{Re}(\bullet)$ denotes the real part of \bullet , and the consistent initial conditions are given by

$$B(x, 0) = B_0(x), \quad \rho(x, 0) = \rho_0(x), \quad u(x, 0) = u_0(x), \quad \phi(x, 0) = |B_0(x)|^2, \quad x \in \Omega. \quad (2.5)$$

Theorem 2.1. *With the periodic boundary conditions, the system (2.4)-(2.5) conserves the following invariants*

$$H_1(x, t) = H_1(x, 0), \quad H_1(x, t) = \phi(x, t) - |B(x, t)|^2, \quad x \in \Omega, \quad t \geq 0, \quad (2.6)$$

$$\mathcal{E}(t) \equiv \mathcal{E}(0), \quad t \geq 0, \quad (2.7)$$

where $\mathcal{E}(t)$ is defined by (2.3).

Proof. With noting the initial condition (2.5) and the fourth equality of (2.4), we have

$$\partial_t H_1(x, t) = \partial_t(\phi(x, t) - |B(x, t)|^2) = \phi_t(x, t) - 2\text{Re}(B_x(x, t) \cdot \bar{B}(x, t)) = 0,$$

which leads to (2.6).

Based on the periodic boundary conditions and (2.4), we can deduce that

$$\begin{aligned} \frac{d\mathcal{E}}{dt} &= 2\omega \text{Re}(B_{xx}, B_t) - \kappa(u_t - \frac{1}{2}\nu\rho_t + \frac{q}{2}\phi_t, \phi) - \kappa(u - \frac{1}{2}\nu\rho + \frac{q}{2}\phi, \phi_t) \\ &\quad - \beta(\rho, \rho_t) - (u, u_t) + \nu(u_t, \rho) + \nu(u, \rho_t) \\ &= 2\omega \text{Re}(B_{xx}, B_t) - \kappa(u - \frac{1}{2}\nu\rho + q\phi, \phi_t) \\ &\quad + (-\beta\rho + \nu u + \frac{1}{2}\kappa\nu\phi, \rho_t) + (-u + \nu\rho - \kappa\phi, u_t) \\ &= 2\text{Re}(\omega B_{xx} - \kappa(u - \frac{1}{2}\nu\rho + q\phi)B, B_t) + (-\beta\rho + \nu u + \frac{1}{2}\kappa\nu\phi, \rho_t) + (-u + \nu\rho - \kappa\phi, u_t) \\ &= -2\text{Re}(iB_t, B_t) + \left(\frac{\delta\mathcal{E}}{\delta\rho}, \rho_t\right) + \left(\frac{\delta\mathcal{E}}{\delta u}, u_t\right) \\ &= \left(\frac{\delta\mathcal{E}}{\delta\rho}, \partial_x \frac{\delta\mathcal{E}}{\delta u}\right) + \left(\frac{\delta\mathcal{E}}{\delta u}, \partial_x \frac{\delta\mathcal{E}}{\delta\rho}\right) \\ &= 0. \end{aligned}$$

This implies the desired result (2.7) and the proof is completed. \square

Theorem 2.2. *Under the the periodic boundary conditions, the system (2.4)-(2.5) conserves the mass (1.3) and the two linear invariants (1.5).*

Proof. With the periodic boundary conditions, we can deduce from the second and third equality of (2.4), respectively, that

$$\begin{aligned}\frac{d}{dt}\mathcal{M}(t) &= 2\text{Re} \int_{\Omega} B_t \cdot \bar{B} dx = 2\text{Re} \int_{\Omega} i \left(\omega |B_x|^2 - \kappa \left(u - \frac{1}{2} \nu \rho + q\phi \right) |B|^2 \right) dx = 0, \\ \frac{d}{dt}\mathcal{I}_1(t) &= \int_{\Omega} \rho_t dx = \int_{\Omega} \partial_x \left(-u + \nu \rho - \kappa \phi \right) dx = 0, \\ \frac{d}{dt}\mathcal{I}_2(t) &= \int_{\Omega} u_t dx = \int_{\Omega} \partial_x \left(-\beta \rho + \nu u + \frac{1}{2} \kappa \nu \phi \right) dx = 0.\end{aligned}$$

This completes the proof. \square

3. High-order energy-preserving scheme

In this section, we will propose a novel class of high-order energy-preserving schemes, which are based on the Fourier pseudo-spectral method in space and the symplectic RK method in time for the reformulated system (2.4), respectively.

3.1. Spatial semi-discretization

Let $\Omega_h = \{x_j | x_j = a + jh, 0 \leq j \leq N\}$ be a partition of Ω with mesh size $h = (b - a)/N$, where N is an even number. Denote $\mathbb{V}_h = \{\mathbf{U} | \mathbf{U} = (U_0, U_1, \dots, U_{N-1})^T\}$ be the space of mesh functions on Ω_h that satisfy the periodic boundary condition $U_{j+N} = U_j$, $j = 0, 1, 2, \dots, N-1$. Define the discrete inner product and norms as

$$\langle \mathbf{U}, \mathbf{V} \rangle_h = h \sum_{j=0}^{N-1} U_j \bar{V}_j, \quad \|\mathbf{U}\|_h = \langle \mathbf{U}, \mathbf{U} \rangle_h^{\frac{1}{2}}, \quad \|\mathbf{U}\|_{h,\infty} = \max_{0 \leq j \leq N-1} |U_j|, \quad \forall \mathbf{U}, \mathbf{V} \in \mathbb{V}_h.$$

We also denote ‘ \cdot ’ as the componentwise product of vectors $\mathbf{U}, \mathbf{V} \in \mathbb{V}_h$, i.e.,

$$\mathbf{U} \cdot \mathbf{V} = (U_0 V_0, U_1 V_1, \dots, U_{N-1} V_{N-1})^T.$$

For brevity, we denote $\mathbf{U} \cdot \mathbf{U}$ and $\mathbf{U} \cdot \bar{\mathbf{U}}$ as U^2 and $|U|^2$, respectively.

Let $X_j(x)$ is the interpolation basis function given by

$$X_j(x) = \frac{1}{N} \sum_{l=-N/2}^{N/2} \frac{1}{a_l} e^{il\mu(x-x_j)},$$

with $a_l = \begin{cases} 1, & |l| < \frac{N}{2}, \\ 2, & |l| = \frac{N}{2}, \end{cases}$ and $\mu = \frac{2\pi}{b-a}$. Then, we denote

$$S_N = \text{span}\{X_j(x), 0 \leq j \leq N-1\}$$

be the interpolation space, and the interpolation operator $I_N : C(\Omega) \rightarrow S_N$ is defined, as follows [5]

$$I_N U(x, t) = \sum_{k=0}^{N-1} U_k(t) X_k(x),$$

where $U_k(t) = U(x_k, t)$. Taking the partial derivative with respect to x , and it follows from the resulting expression at the collocation point x_j that

$$\frac{\partial^m I_N U(x_j)}{\partial x^m} = \sum_{k=0}^{N-1} U_k \frac{d^m X_k(x_j)}{dx^m} = (\mathcal{D}_m \mathbf{U})_j, \quad \mathbf{U} \in \mathbb{V}_h,$$

where $j = 0, \dots, N-1$ and \mathcal{D}_m is an $N \times N$ matrix with elements given by

$$(\mathcal{D}_m)_{j,k} = \frac{d^m X_k(x_j)}{dx^m}, \quad j, k = 0, 1, \dots, N-1.$$

In particular, for \mathcal{D}_1 and \mathcal{D}_2 we have

$$\mathcal{D}_1 = \mathcal{F}_N^H \Lambda^1 \mathcal{F}_N, \quad \Lambda^1 = i\mu \cdot \text{diag}(0, 1, \dots, \frac{N}{2} - 1, 0, -\frac{N}{2} + 1, \dots, -1), \quad (3.1)$$

$$\mathcal{D}_2 = \mathcal{F}_N^H \Lambda^2 \mathcal{F}_N, \quad \Lambda^2 = [i\mu \cdot \text{diag}(0, 1, \dots, \frac{N}{2} - 1, \frac{N}{2}, -\frac{N}{2} + 1, \dots, -1)]^2, \quad (3.2)$$

where \mathcal{F}_N is the discrete Fourier transform matrix with elements $(\mathcal{F}_N)_{j,k} = \frac{1}{\sqrt{N}} e^{-ijk \frac{2\pi}{N}}$, \mathcal{F}_N^H is the conjugate transpose matrix of \mathcal{F}_N . For more details, please refer to [30].

Applying the standard Fourier pseudo-spectral method to approximate the equation (2.4) in space yields

$$\begin{cases} \frac{d}{dt} \mathbf{B} = i(\omega \mathcal{D}_2 \mathbf{B} - \kappa(\mathbf{u} - \frac{1}{2} \nu \boldsymbol{\rho} + q\phi) \cdot \mathbf{B}), \\ \frac{d}{dt} \boldsymbol{\rho} = \mathcal{D}_1(-\mathbf{u} + \nu \boldsymbol{\rho} - \kappa\phi), \\ \frac{d}{dt} \mathbf{u} = \mathcal{D}_1(-\beta \boldsymbol{\rho} + \nu \mathbf{u} + \frac{1}{2} \kappa \nu \phi), \\ \frac{d}{dt} \phi = 2\text{Re}(\mathbf{B}_t \cdot \bar{\mathbf{B}}). \end{cases} \quad (3.3)$$

Then, the discrete conservation laws of the above semi-discrete scheme will be given in the following theorems.

Theorem 3.1. *The semi-discrete system (3.3) preserves the following semi-discrete invariants*

- *Mass*

$$\mathcal{M}_h(t) = \mathcal{M}_h(0), \quad \mathcal{M}_h = \langle |\mathbf{B}|^2, 1 \rangle_h. \quad (3.4)$$

- *Two quadratic invariants*

$$\mathbf{H}_1(t) = \mathbf{H}_1(0), \quad \mathcal{E}_h(t) = \mathcal{E}_h(0), \quad (3.5)$$

where

$$\begin{aligned} \mathbf{H}_1(t) &= \phi(t) - |\mathbf{B}(t)|^2, \\ \mathcal{E}_h(t) &= \omega \langle \mathcal{D}_2 \mathbf{B}, \mathbf{B} \rangle_h - \kappa \langle \mathbf{u} - \frac{\nu}{2} \boldsymbol{\rho} + \frac{q}{2} \phi, \phi \rangle_h - \frac{\beta}{2} \langle \boldsymbol{\rho}, \boldsymbol{\rho} \rangle_h - \frac{1}{2} \langle \mathbf{u}, \mathbf{u} \rangle_h + \nu \langle \mathbf{u}, \boldsymbol{\rho} \rangle_h. \end{aligned}$$

- *Two linear invariants*

$$\mathcal{I}_{1h}(t) = \mathcal{I}_{1h}(0), \quad \mathcal{I}_{2h}(t) = \mathcal{I}_{2h}(0), \quad (3.6)$$

where

$$\mathcal{I}_{1h} = \langle \boldsymbol{\rho}, 1 \rangle_h, \quad \mathcal{I}_{2h} = \langle \mathbf{u}, 1 \rangle_h.$$

Proof. The proof is similar to that of Theorem 2.1 and we omit it here for brevity. \square

3.2. Full discretization

Let $t_n = n\tau$ and $t_{ni} = n\tau + c_i\tau$, $n = 0, 1, 2, \dots$, $i = 1, 2, \dots, s$, where τ is the time step. Let W_j^n and $(W_{ni})_j$ be the numerical approximation to the function $W(x, t)$ at points (x_j, t_n) and (x_j, t_{ni}) where $j = 0, 1, 2, \dots, N-1$ and $n = 0, 1, 2, \dots$, respectively. Using an s -stage RK method to discrete the semi-discrete system (3.3) in time, we then obtain the following fully discrete scheme.

Scheme 3.1 (FPRK- s scheme). Consider an s -stages RK method (A, b, c) can be described by the coefficients matrix $A = (a_{ij})_{i,j=1}^s \in \mathbb{R}^{s \times s}$, the weight vector $b = (b_1, \dots, b_s)^T \in \mathbb{R}^s$ and the abscissa $c = (c_1, \dots, c_s)^T \in \mathbb{R}^s$. For given $(B^n, \rho^n, u^n, \phi^n)$, the intermediate values are obtained by

$$\begin{cases} B_{ni} = B^n + \tau \sum_{j=1}^s a_{ij} k_j^1, & k_i^1 = i(\omega \mathcal{D}_2 B_{ni} - \kappa(u_{ni} - \frac{1}{2}\nu \rho_{ni} + q\phi_{ni}) \cdot B_{ni}), \\ \rho_{ni} = \rho^n + \tau \sum_{j=1}^s a_{ij} k_j^2, & k_i^2 = \mathcal{D}_1(-u_{ni} + \nu \rho_{ni} - \kappa \phi_{ni}), \\ u_{ni} = u^n + \tau \sum_{j=1}^s a_{ij} k_j^3, & k_i^3 = \mathcal{D}_1(-\beta \rho_{ni} + \nu u_{ni} + \frac{1}{2}\kappa \nu \phi_{ni}), \\ \phi_{ni} = \phi^n + \tau \sum_{j=1}^s a_{ij} k_j^4, & k_i^4 = 2\text{Re}(\bar{B}_{ni} \cdot k_i^1), \quad i = 1, 2, \dots, s. \end{cases} \quad (3.7)$$

Then $(B^{n+1}, \rho^{n+1}, u^{n+1}, \phi^{n+1})$ is calculated via

$$B^{n+1} = B^n + \tau \sum_{i=1}^s b_i k_i^1, \quad (3.8)$$

$$\rho^{n+1} = \rho^n + \tau \sum_{i=1}^s b_i k_i^2, \quad (3.9)$$

$$u^{n+1} = u^n + \tau \sum_{i=1}^s b_i k_i^3, \quad (3.10)$$

$$\phi^{n+1} = \phi^n + \tau \sum_{i=1}^s b_i k_i^4. \quad (3.11)$$

Theorem 3.2. If the coefficients of the RK method (3.7)-(3.11) satisfy the following condition

$$b_i a_{ij} + b_j a_{ji} = b_i b_j, \quad \forall i, j = 1, \dots, s, \quad (3.12)$$

then the FPRK- s scheme conserves the following invariants:

- The discrete mass

$$\mathcal{M}_h^{n+1} = \mathcal{M}_h^n, \quad \mathcal{M}_h^n = \langle |B^n|^2, 1 \rangle_h, \quad n = 0, 1, 2, \dots, \quad (3.13)$$

- Two discrete quadratic invariants

$$H_{1,h}^{n+1} = H_{1,h}^n, \quad \mathcal{E}_h^{n+1} = \mathcal{E}_h^n, \quad n = 0, 1, 2, \dots, \quad (3.14)$$

where

$$\begin{aligned} H_{1,h}^n &= \phi^n - |B^n|^2, \\ \mathcal{E}_h^n &= \omega \langle \mathcal{D}_2 B^n, B^n \rangle_h - \kappa \langle u^n - \frac{\nu}{2} \rho^n + \frac{q}{2} \phi^n, \phi^n \rangle_h - \frac{\beta}{2} \langle \rho^n, \rho^n \rangle_h - \frac{1}{2} \langle u^n, u^n \rangle_h + \nu \langle u^n, \rho^n \rangle_h. \end{aligned}$$

Proof. It follows from Eq. (3.8) that

$$\mathcal{M}_h^{n+1} - \mathcal{M}_h^n = \tau \sum_{i=1}^s b_i \langle B^n, k_i^1 \rangle_h + \tau \sum_{i=1}^s b_i \langle k_i^1, B^n \rangle_h + \tau^2 \sum_{i,j=1}^s b_i b_j \langle k_i^1, k_j^1 \rangle_h. \quad (3.15)$$

Substituting $B^n = B_{ni} - \tau \sum_{j=1}^s a_{ij} k_j^1$ into (3.15) yields

$$\begin{aligned} \mathcal{M}_h^{n+1} - \mathcal{M}_h^n &= \tau \sum_{i=1}^s b_i \langle B_{ni}, k_i^1 \rangle_h + \tau \sum_{i=1}^s b_i \langle k_i^1, B_{ni} \rangle_h + \tau^2 \sum_{i,j=1}^s (b_i b_j - b_i a_{ij} - b_j a_{ji}) \langle k_i^1, k_j^1 \rangle_h \\ &= \tau \sum_{i=1}^s b_i \langle B_{ni}, k_i^1 \rangle_h + \tau \sum_{i=1}^s b_i \langle k_i^1, B_{ni} \rangle_h, \end{aligned} \quad (3.16)$$

where the condition (3.12) is used. Furthermore, we arrive at

$$\begin{aligned}
& \tau \sum_{i=1}^s b_i \langle \mathbf{B}_{ni}, k_i^1 \rangle_h + \tau \sum_{i=1}^s b_i \langle k_i^1, \mathbf{B}_{ni} \rangle_h \\
&= 2\tau \sum_{i=1}^s b_i \operatorname{Re} \langle k_i^1, \mathbf{B}_{ni} \rangle_h \\
&= 2\tau \sum_{i=1}^s b_i \operatorname{Re} \left(i\omega \langle \mathcal{D}_2 \mathbf{B}_{ni}, \mathbf{B}_{ni} \rangle_h - i\kappa \langle \mathbf{u}_{ni} - \frac{1}{2} \nu \rho_{ni} + q\phi_{ni}, |\mathbf{B}_{ni}|^2 \rangle_h \right) \\
&= 0.
\end{aligned}$$

Combining the above result with (3.16), we get the discrete mass (3.13).

Based on (3.8), (3.12) and $\mathbf{B}^n = \mathbf{B}_{ni} - \tau \sum_{j=1}^s a_{ij} k_j^1$, we get

$$\begin{aligned}
|\mathbf{B}^{n+1}|^2 - |\mathbf{B}^n|^2 &= \mathbf{B}^{n+1} \cdot \bar{\mathbf{B}}^{n+1} - \mathbf{B}^n \cdot \bar{\mathbf{B}}^n \\
&= \tau \sum_{i=1}^s b_i (k_i^1 \cdot \bar{\mathbf{B}}^n) + \tau \sum_{i=1}^s b_i (\bar{k}_i^1 \cdot \mathbf{B}^n) + \tau^2 \sum_{i,j=1}^s b_i b_j (k_i^1 \cdot \bar{k}_j^1) \\
&= \tau \sum_{i=1}^s b_i (k_i^1 \cdot \bar{\mathbf{B}}_{ni}) + \tau \sum_{i=1}^s b_i (\bar{k}_i^1 \cdot \mathbf{B}_{ni}) + \tau^2 \sum_{i,j=1}^s (b_i b_j - b_i a_{ij} - b_j a_{ji}) (k_i^1 \cdot \bar{k}_j^1) \\
&= \tau \sum_{i=1}^s b_i (k_i^1 \cdot \bar{\mathbf{B}}_{ni}) + \tau \sum_{i=1}^s b_i (\bar{k}_i^1 \cdot \mathbf{B}_{ni}). \tag{3.17}
\end{aligned}$$

Noticing that

$$\phi^{n+1} - \phi^n = \tau \sum_{i=1}^s b_i k_i^4 = 2\tau \sum_{i=1}^s b_i \operatorname{Re} (k_i^1 \cdot \bar{\mathbf{B}}_{ni}) = \tau \sum_{i=1}^s b_i (k_i^1 \cdot \bar{\mathbf{B}}_{ni}) + \tau \sum_{i=1}^s b_i (\bar{k}_i^1 \cdot \mathbf{B}_{ni}). \tag{3.18}$$

It follows from (3.17) and (3.18), together with $\phi^0 - |\mathbf{B}^0|^2$ that

$$\phi^{n+1} - |\mathbf{B}^{n+1}|^2 = \phi^n - |\mathbf{B}^n|^2, \quad n = 0, 1, 2, \dots, \tag{3.19}$$

which implies the first equality of (3.14).

Similar to Eq. (3.16), we can obtain from **Scheme 3.1** that

$$\begin{aligned}
\langle \mathcal{D}_2 \mathbf{B}^{n+1}, \mathbf{B}^{n+1} \rangle_h - \langle \mathcal{D}_2 \mathbf{B}^n, \mathbf{B}^n \rangle_h &= 2\tau \sum_{i=1}^s b_i \operatorname{Re} \langle \mathcal{D}_2 \mathbf{B}_{ni}, k_i^1 \rangle_h, \\
\langle \mathbf{u}^{n+1}, \phi^{n+1} \rangle_h - \langle \mathbf{u}^n, \phi^n \rangle_h &= \tau \sum_{i=1}^s b_i (\langle k_i^3, \phi_{ni} \rangle_h + \langle \mathbf{u}_{ni}, k_i^4 \rangle_h), \\
\langle \rho^{n+1}, \phi^{n+1} \rangle_h - \langle \rho^n, \phi^n \rangle_h &= \tau \sum_{i=1}^s b_i (\langle k_i^2, \phi_{ni} \rangle_h + \langle \rho_{ni}, k_i^4 \rangle_h), \\
\langle \phi^{n+1}, \phi^{n+1} \rangle_h - \langle \phi^n, \phi^n \rangle_h &= 2\tau \sum_{i=1}^s b_i \langle \phi_{ni}, k_i^4 \rangle_h, \\
\langle \rho^{n+1}, \rho^{n+1} \rangle_h - \langle \rho^n, \rho^n \rangle_h &= 2\tau \sum_{i=1}^s b_i \langle \rho_{ni}, k_i^2 \rangle_h, \\
\langle \mathbf{u}^{n+1}, \mathbf{u}^{n+1} \rangle_h - \langle \mathbf{u}^n, \mathbf{u}^n \rangle_h &= 2\tau \sum_{i=1}^s b_i \langle \mathbf{u}_{ni}, k_i^3 \rangle_h, \\
\langle \mathbf{u}^{n+1}, \rho^{n+1} \rangle_h - \langle \mathbf{u}^n, \rho^n \rangle_h &= \tau \sum_{i=1}^s b_i (\langle k_i^3, \rho_{ni} \rangle_h + \langle \mathbf{u}_{ni}, k_i^2 \rangle_h).
\end{aligned}$$

Thus, combining the above equations and (3.7), together with $k_i^4 = 2\text{Re}(\bar{\mathbf{B}}_{ni} \cdot k_i^1)$, we can derive

$$\begin{aligned}
& \mathcal{E}_h^{n+1} - \mathcal{E}_h^n \\
&= \tau \sum_{i=1}^s b_i \left[2\omega \text{Re} \langle \mathcal{D}_2 \mathbf{B}_{ni}, k_i^1 \rangle_h - \kappa (\langle k_i^3, \phi_{ni} \rangle_h + \langle \mathbf{u}_{ni}, k_i^4 \rangle_h) + \frac{\kappa\nu}{2} (\langle k_i^2, \phi_{ni} \rangle_h + \langle \rho_{ni}, k_i^4 \rangle_h) \right. \\
&\quad \left. - \kappa q \langle \phi_{ni}, k_i^4 \rangle_h - \beta \langle \rho_{ni}, k_i^2 \rangle_h - \langle \mathbf{u}_{ni}, k_i^3 \rangle_h + \nu (\langle k_i^3, \rho_{ni} \rangle_h + \langle \mathbf{u}_{ni}, k_i^2 \rangle_h) \right] \\
&= \tau \sum_{i=1}^s b_i \left[2\text{Re} \langle \omega \mathcal{D}_2 \mathbf{B}_{ni} - \kappa (\mathbf{u}_{ni} - \frac{\nu}{2} \rho_{ni} + q \phi_{ni}) \cdot \mathbf{B}_{ni}, k_i^1 \rangle_h + \langle -\mathbf{u}_{ni} + \nu \rho_{ni} - \kappa \phi_{ni}, k_i^3 \rangle_h \right. \\
&\quad \left. + \langle -\beta \rho_{ni} + \nu \mathbf{u}_{ni} + \frac{1}{2} \kappa \nu \phi_{ni}, k_i^2 \rangle_h \right] \\
&= \tau \sum_{i=1}^s b_i \left[-2\text{Re} \langle i k_i^1, k_i^1 \rangle_h + \langle -\mathbf{u}_{ni} + \nu \rho_{ni} - \kappa \phi_{ni}, \mathcal{D}_1 (-\beta \rho_{ni} + \nu \mathbf{u}_{ni} + \frac{1}{2} \kappa \nu \phi_{ni}) \rangle_h \right. \\
&\quad \left. + \langle -\beta \rho_{ni} + \nu \mathbf{u}_{ni} + \frac{1}{2} \kappa \nu \phi_{ni}, \mathcal{D}_1 (-\mathbf{u}_{ni} + \nu \rho_{ni} - \kappa \phi_{ni}) \rangle_h \right] \\
&= 0.
\end{aligned}$$

This immediately gives the second equality of (3.14). The proof is completed. \square

Remark 3.1. With (3.13), one can deduce that the **Scheme 3.1** can conserve the discrete Hamiltonian energy, as follows:

$$\mathcal{H}_h^{n+1} = \mathcal{H}_h^n, \quad n = 0, 1, 2, \dots, \quad (3.20)$$

where

$$\mathcal{H}_h^n = \omega \langle \mathcal{D}_2 \mathbf{B}^n, \mathbf{B}^n \rangle_h - \kappa \langle \mathbf{u}^n - \frac{\nu}{2} \rho^n + \frac{q}{2} |\mathbf{B}^n|^2, |\mathbf{B}^n|^2 \rangle_h - \frac{\beta}{2} \langle \rho^n, \rho^n \rangle_h - \frac{1}{2} \langle \mathbf{u}^n, \mathbf{u}^n \rangle_h + \nu \langle \mathbf{u}^n, \rho^n \rangle_h.$$

Theorem 3.3. For any RK method, the FPRK-s scheme conserves the two discrete linear invariants, as follows:

$$\mathcal{I}_{1h}^{n+1} = \mathcal{I}_{1h}^n, \quad \mathcal{I}_{2h}^{n+1} = \mathcal{I}_{2h}^n, \quad (3.21)$$

where

$$\mathcal{I}_{1h}^n = \langle \rho^n, 1 \rangle_h, \quad \mathcal{I}_{2h}^n = \langle \mathbf{u}^n, 1 \rangle_h.$$

Proof. According to (3.9)-(3.10), we obtain

$$\begin{aligned}
\mathcal{I}_{1h}^{n+1} - \mathcal{I}_{1h}^n &= \tau \sum_{i=1}^s b_i \langle k_i^2, 1 \rangle_h = \tau \sum_{i=1}^s b_i \langle \mathcal{D}_1 (-\mathbf{u}_{ni} + \nu \rho_{ni} - \kappa \phi_{ni}), 1 \rangle_h = 0, \\
\mathcal{I}_{2h}^{n+1} - \mathcal{I}_{2h}^n &= \tau \sum_{i=1}^s b_i \langle k_i^3, 1 \rangle_h = \tau \sum_{i=1}^s b_i \langle \mathcal{D}_1 (-\beta \rho_{ni} + \nu \mathbf{u}_{ni} + \frac{1}{2} \kappa \nu \phi_{ni}), 1 \rangle_h = 0.
\end{aligned}$$

This completes the proof. \square

Remark 3.2. It is well known that the Gaussian collocation methods [12, 28] satisfy the condition (3.12), so they can be used to develop arbitrarily high-order energy-preserving methods based on our theory.

$$\begin{aligned}
\left. \begin{array}{c} c \\ b^T \end{array} \right| A &= \left. \begin{array}{c} \frac{1}{2} \\ \frac{1}{2} \end{array} \right| \frac{1}{1}, \quad \left. \begin{array}{c} c \\ b^T \end{array} \right| A = \left. \begin{array}{c} \frac{1}{2} - \frac{\sqrt{3}}{6} \\ \frac{1}{2} + \frac{\sqrt{3}}{6} \end{array} \right| \left. \begin{array}{c} \frac{1}{4} \\ \frac{1}{4} + \frac{\sqrt{3}}{6} \end{array} \right| \frac{1}{\frac{1}{2}}, \\
\left. \begin{array}{c} c \\ b^T \end{array} \right| A &= \left. \begin{array}{c} \frac{1}{2} - \frac{\sqrt{15}}{10} \\ \frac{1}{2} + \frac{\sqrt{15}}{10} \end{array} \right| \left. \begin{array}{c} \frac{5}{36} \\ \frac{5}{36} + \frac{\sqrt{15}}{24} \end{array} \right| \left. \begin{array}{c} \frac{2}{9} - \frac{\sqrt{15}}{15} \\ \frac{2}{9} + \frac{\sqrt{15}}{15} \end{array} \right| \left. \begin{array}{c} \frac{5}{36} - \frac{\sqrt{15}}{30} \\ \frac{5}{36} - \frac{\sqrt{15}}{24} \end{array} \right| \frac{5}{18}.
\end{aligned}$$

Table 1: The coefficients of the Gaussian collocation methods of order 2 (s=1), 4 (s=2) and 6 (s=3).

Remark 3.3. As the Gaussian collocation method of order 2 (see Table (1)) is chosen, the **Scheme 3.1** reduced to the CN-FP scheme [38], as follows:

$$\begin{cases} i\delta_t \mathbf{B}^n + \omega \mathcal{D}_2 \mathbf{B}^{n+\frac{1}{2}} - \kappa(\mathbf{u}^{n+\frac{1}{2}} - \frac{1}{2}\nu \boldsymbol{\rho}^{n+\frac{1}{2}} + \frac{q}{2}(|\mathbf{B}^{n+1}|^2 + |\mathbf{B}^n|^2)) \cdot \mathbf{B}^{n+\frac{1}{2}} = 0, \\ \delta_t \boldsymbol{\rho}^n + \mathcal{D}_1(\mathbf{u}^{n+\frac{1}{2}} - \nu \boldsymbol{\rho}^{n+\frac{1}{2}} + \frac{\kappa}{2}(|\mathbf{B}^{n+1}|^2 + |\mathbf{B}^n|^2)) = 0, \\ \delta_t \mathbf{u}^n + \mathcal{D}_1(\beta \boldsymbol{\rho}^{n+\frac{1}{2}} - \nu \mathbf{u}^{n+\frac{1}{2}} - \frac{\kappa\nu}{4}(|\mathbf{B}^{n+1}|^2 + |\mathbf{B}^n|^2)) = 0, \quad n = 0, 1, 2, \dots, \end{cases} \quad (3.22)$$

where

$$\delta_t \mathbf{U}^n = \frac{\mathbf{U}^{n+1} - \mathbf{U}^n}{\tau}, \quad \mathbf{U}^{n+\frac{1}{2}} = \frac{\mathbf{U}^{n+1} + \mathbf{U}^n}{2}, \quad \mathbf{U}^n \in \mathbb{V}_h.$$

4. A fast solver for the proposed scheme

Inspired by [9, 36], we propose an efficient fixed pointed iteration solver for solving the nonlinear equations of the **Scheme 3.1** in this section. For convenience, we only take the proposed FPRK-2 scheme into consideration, in which the RK coefficients are presented in Table 1.

For given \mathbf{B}^n , $\boldsymbol{\rho}^n$, \mathbf{u}^n and ϕ^n , together with the first equality (3.14), the proposed FPRK-2 scheme can be rewritten as

$$k_1^1 = i(\omega \mathcal{D}_2 \mathbf{B}_{n1} - \kappa(\mathbf{u}_{n1} - \frac{1}{2}\nu \boldsymbol{\rho}_{n1} + q\phi_{n1}) \cdot \mathbf{B}_{n1}), \quad (4.1)$$

$$k_2^1 = i(\omega \mathcal{D}_2 \mathbf{B}_{n2} - \kappa(\mathbf{u}_{n2} - \frac{1}{2}\nu \boldsymbol{\rho}_{n2} + q\phi_{n2}) \cdot \mathbf{B}_{n2}), \quad (4.2)$$

$$k_1^2 = \mathcal{D}_1(-\mathbf{u}_{n1} + \nu \boldsymbol{\rho}_{n1} - \kappa\phi_{n1}), \quad k_2^2 = \mathcal{D}_1(-\mathbf{u}_{n2} + \nu \boldsymbol{\rho}_{n2} - \kappa\phi_{n2}), \quad (4.3)$$

$$k_1^3 = \mathcal{D}_1(-\beta \boldsymbol{\rho}_{n1} + \nu \mathbf{u}_{n1} + \frac{\kappa\nu}{2}\phi_{n1}), \quad k_2^3 = \mathcal{D}_1(-\beta \boldsymbol{\rho}_{n2} + \nu \mathbf{u}_{n2} + \frac{\kappa\nu}{2}\phi_{n2}), \quad (4.4)$$

where

$$\mathbf{B}_{n1} = \mathbf{B}^n + \tau(a_{11}k_1^1 + a_{12}k_2^1), \quad \mathbf{B}_{n2} = \mathbf{B}^n + \tau(a_{21}k_1^1 + a_{22}k_2^1), \quad (4.5)$$

$$\boldsymbol{\rho}_{n1} = \boldsymbol{\rho}^n + \tau(a_{11}k_1^2 + a_{12}k_2^2), \quad \boldsymbol{\rho}_{n2} = \boldsymbol{\rho}^n + \tau(a_{21}k_1^2 + a_{22}k_2^2), \quad (4.6)$$

$$\mathbf{u}_{n1} = \mathbf{u}^n + \tau(a_{11}k_1^3 + a_{12}k_2^3), \quad \mathbf{u}_{n2} = \mathbf{u}^n + \tau(a_{21}k_1^3 + a_{22}k_2^3), \quad (4.7)$$

$$\phi_{n1} = |\mathbf{B}^n|^2 + 2\tau(a_{11}\text{Re}(\bar{\mathbf{B}}_{n1} \cdot k_1^1) + a_{12}\text{Re}(\bar{\mathbf{B}}_{n2} \cdot k_2^1)), \quad (4.8)$$

$$\phi_{n2} = |\mathbf{B}^n|^2 + 2\tau(a_{21}\text{Re}(\bar{\mathbf{B}}_{n1} \cdot k_1^1) + a_{22}\text{Re}(\bar{\mathbf{B}}_{n2} \cdot k_2^1)). \quad (4.9)$$

Then, \mathbf{B}^{n+1} , $\boldsymbol{\rho}^{n+1}$ and \mathbf{u}^{n+1} are updated by

$$\mathbf{B}^{n+1} = \mathbf{B}^n + \tau b_1 k_1^1 + \tau b_2 k_2^1, \quad (4.10)$$

$$\boldsymbol{\rho}^{n+1} = \boldsymbol{\rho}^n + \tau b_1 k_1^2 + \tau b_2 k_2^2, \quad (4.11)$$

$$\mathbf{u}^{n+1} = \mathbf{u}^n + \tau b_1 k_1^3 + \tau b_2 k_2^3. \quad (4.12)$$

In light of (4.1)-(4.2) and (4.5), it holds that

$$\begin{bmatrix} 1 - i\tau\omega a_{11}\mathcal{D}_2 & -i\tau\omega a_{12}\mathcal{D}_2 \\ -i\tau\omega a_{21}\mathcal{D}_2 & 1 - i\tau\omega a_{22}\mathcal{D}_2 \end{bmatrix} \begin{bmatrix} k_1^1 \\ k_2^1 \end{bmatrix} = \begin{bmatrix} F_1^n \\ F_2^n \end{bmatrix}, \quad (4.13)$$

where

$$F_k^n = i\omega \mathcal{D}_2 \mathbf{B}^n - i\kappa(\mathbf{u}_{nk} - \frac{1}{2}\nu \boldsymbol{\rho}_{nk} + q\phi_{nk}) \cdot \mathbf{B}_{nk}, \quad k = 1, 2.$$

Meanwhile, we can obtain from (4.3)-(4.4), (4.6) and (4.7) that

$$\begin{bmatrix} 1 - \nu\tau a_{11}\mathcal{D}_1 & -\nu\tau a_{12}\mathcal{D}_1 & \tau a_{11}\mathcal{D}_1 & \tau a_{12}\mathcal{D}_1 \\ -\nu\tau a_{21}\mathcal{D}_1 & 1 - \nu\tau a_{22}\mathcal{D}_1 & \tau a_{21}\mathcal{D}_1 & \tau a_{22}\mathcal{D}_1 \\ \beta\tau a_{11}\mathcal{D}_1 & \beta\tau a_{12}\mathcal{D}_1 & 1 - \nu\tau a_{11}\mathcal{D}_1 & -\nu\tau a_{12}\mathcal{D}_1 \\ \beta\tau a_{21}\mathcal{D}_1 & \beta\tau a_{22}\mathcal{D}_1 & -\nu\tau a_{21}\mathcal{D}_1 & 1 - \nu\tau a_{22}\mathcal{D}_1 \end{bmatrix} \begin{bmatrix} k_1^2 \\ k_2^2 \\ k_1^3 \\ k_2^3 \end{bmatrix} = \begin{bmatrix} \mathcal{D}_1 \chi_1^n \\ \mathcal{D}_1 \chi_2^n \\ \mathcal{D}_1 \chi_3^n \\ \mathcal{D}_1 \chi_4^n \end{bmatrix} \quad (4.14)$$

with

$$\begin{aligned}\chi_1^n &= -\mathbf{u}^n + \nu \boldsymbol{\rho}^n - \kappa \phi_{n1}, \quad \chi_2^n = -\mathbf{u}^n + \nu \boldsymbol{\rho}^n - \kappa \phi_{n2}, \\ \chi_3^n &= -\beta \boldsymbol{\rho}^n + \nu \mathbf{u}^n + \frac{\kappa \nu}{2} \phi_{n1}, \quad \chi_4^n = -\beta \boldsymbol{\rho}^n + \nu \mathbf{u}^n + \frac{\kappa \nu}{2} \phi_{n2}.\end{aligned}$$

For the nonlinear equations (4.13) and (4.14), we apply the fixed-point iteration strategy, as follows:

$$\begin{bmatrix} 1 - i\tau\omega a_{11}\mathcal{D}_2 & -i\tau\omega a_{12}\mathcal{D}_2 \\ -i\tau\omega a_{21}\mathcal{D}_2 & 1 - i\tau\omega a_{22}\mathcal{D}_2 \end{bmatrix} \begin{bmatrix} (k_1^1)^{l+1} \\ (k_2^1)^{l+1} \end{bmatrix} = \begin{bmatrix} F_1^{n,l} \\ F_2^{n,l} \end{bmatrix}, \quad (4.15)$$

and

$$\begin{bmatrix} 1 - \nu\tau a_{11}\mathcal{D}_1 & -\nu\tau a_{12}\mathcal{D}_1 & \tau a_{11}\mathcal{D}_1 & \tau a_{12}\mathcal{D}_1 \\ -\nu\tau a_{21}\mathcal{D}_1 & 1 - \nu\tau a_{22}\mathcal{D}_1 & \tau a_{21}\mathcal{D}_1 & \tau a_{22}\mathcal{D}_1 \\ \beta\tau a_{11}\mathcal{D}_1 & \beta\tau a_{12}\mathcal{D}_1 & 1 - \nu\tau a_{11}\mathcal{D}_1 & -\nu\tau a_{12}\mathcal{D}_1 \\ \beta\tau a_{21}\mathcal{D}_1 & \beta\tau a_{22}\mathcal{D}_1 & -\nu\tau a_{21}\mathcal{D}_1 & 1 - \nu\tau a_{22}\mathcal{D}_1 \end{bmatrix} \begin{bmatrix} (k_1^2)^{l+1} \\ (k_2^2)^{l+1} \\ (k_1^3)^{l+1} \\ (k_2^3)^{l+1} \end{bmatrix} = \begin{bmatrix} \mathcal{D}_1 \chi_1^{n,l} \\ \mathcal{D}_1 \chi_2^{n,l} \\ \mathcal{D}_1 \chi_3^{n,l} \\ \mathcal{D}_1 \chi_4^{n,l} \end{bmatrix}, \quad (4.16)$$

where $l = 0, 1, 2, \dots, M-1$.

Using the equations (3.1) and (3.2) and let $\widetilde{\bullet} = \mathcal{F}_N \bullet$, we can deduce from (4.15) and (4.16) that

$$\begin{bmatrix} 1 - i\tau\omega a_{11}\Lambda^2 & -i\tau\omega a_{12}\Lambda^2 \\ -i\tau\omega a_{21}\Lambda^2 & 1 - i\tau\omega a_{22}\Lambda^2 \end{bmatrix} \begin{bmatrix} \widetilde{(k_1^1)^{l+1}} \\ \widetilde{(k_2^1)^{l+1}} \end{bmatrix} = \begin{bmatrix} \widetilde{F_1^{n,l}} \\ \widetilde{F_2^{n,l}} \end{bmatrix},$$

and

$$\begin{bmatrix} 1 - \nu\tau a_{11}\Lambda^1 & -\nu\tau a_{12}\Lambda^1 & \tau a_{11}\Lambda_j^1 & \tau a_{12}\Lambda^1 \\ -\nu\tau a_{21}\Lambda^1 & 1 - \nu\tau a_{22}\Lambda^1 & \tau a_{21}\Lambda_j^1 & \tau a_{22}\Lambda^1 \\ \beta\tau a_{11}\Lambda^1 & \beta\tau a_{12}\Lambda^1 & 1 - \nu\tau a_{11}\Lambda_j^1 & -\nu\tau a_{12}\Lambda^1 \\ \beta\tau a_{21}\Lambda^1 & \beta\tau a_{22}\Lambda_j^1 & -\nu\tau a_{21}\Lambda^1 & 1 - \nu\tau a_{22}\Lambda^1 \end{bmatrix} \begin{bmatrix} \widetilde{(k_1^2)^{l+1}} \\ \widetilde{(k_2^2)^{l+1}} \\ \widetilde{(k_1^3)^{l+1}} \\ \widetilde{(k_2^3)^{l+1}} \end{bmatrix} = \begin{bmatrix} \Lambda^1 \widetilde{\chi_1^{n,l}} \\ \Lambda^1 \widetilde{\chi_2^{n,l}} \\ \Lambda^1 \widetilde{\chi_3^{n,l}} \\ \Lambda^1 \widetilde{\chi_4^{n,l}} \end{bmatrix},$$

which implies that

$$\begin{bmatrix} 1 - i\tau\omega a_{11}\Lambda_j^2 & -i\tau\omega a_{12}\Lambda_j^2 \\ -i\tau\omega a_{21}\Lambda_j^2 & 1 - i\tau\omega a_{22}\Lambda_j^2 \end{bmatrix} \begin{bmatrix} \widetilde{(k_1^1)_j^{l+1}} \\ \widetilde{(k_2^1)_j^{l+1}} \end{bmatrix} = \begin{bmatrix} \widetilde{F_1^{n,l}_j} \\ \widetilde{F_2^{n,l}_j} \end{bmatrix},$$

and

$$\begin{bmatrix} 1 - \nu\tau a_{11}\Lambda_j^1 & -\nu\tau a_{12}\Lambda_j^1 & \tau a_{11}\Lambda_j^1 & \tau a_{12}\Lambda_j^1 \\ -\nu\tau a_{21}\Lambda_j^1 & 1 - \nu\tau a_{22}\Lambda_j^1 & \tau a_{21}\Lambda_j^1 & \tau a_{22}\Lambda_j^1 \\ \beta\tau a_{11}\Lambda_j^1 & \beta\tau a_{12}\Lambda_j^1 & 1 - \nu\tau a_{11}\Lambda_j^1 & -\nu\tau a_{12}\Lambda_j^1 \\ \beta\tau a_{21}\Lambda_j^1 & \beta\tau a_{22}\Lambda_j^1 & -\nu\tau a_{21}\Lambda_j^1 & 1 - \nu\tau a_{22}\Lambda_j^1 \end{bmatrix} \begin{bmatrix} \widetilde{(k_1^2)_j^{l+1}} \\ \widetilde{(k_2^2)_j^{l+1}} \\ \widetilde{(k_1^3)_j^{l+1}} \\ \widetilde{(k_2^3)_j^{l+1}} \end{bmatrix} = \begin{bmatrix} \Lambda_j^1 \widetilde{(\chi_1^{n,l})_j} \\ \Lambda_j^1 \widetilde{(\chi_2^{n,l})_j} \\ \Lambda_j^1 \widetilde{(\chi_3^{n,l})_j} \\ \Lambda_j^1 \widetilde{(\chi_4^{n,l})_j} \end{bmatrix},$$

where $j = 0, 1, 2, \dots, N-1$.

After we obtain $\widetilde{(k_i^1)^M}$, $\widetilde{(k_i^2)^M}$ and $\widetilde{(k_i^3)^M}$, $(k_i^1)^M$, $(k_i^2)^M$ and $(k_i^3)^M$ are then updated by $\mathcal{F}_N^H \widetilde{(k_i^1)^M}$, $\mathcal{F}_N^H \widetilde{(k_i^2)^M}$ and $\mathcal{F}_N^H \widetilde{(k_i^3)^M}$, $i = 1, 2$, respectively. Finally, \mathbf{B}^{n+1} , $\boldsymbol{\rho}^{n+1}$ and \mathbf{u}^{n+1} are obtained from (4.10)-(4.12). In practical computation, we choose the iterative initial value $(k_i^1)^0 = \mathbf{B}^n$, $(k_i^2)^0 = \boldsymbol{\rho}^n$, $(k_i^3)^0 = \mathbf{u}^n$, $i = 1, 2$ and the iteration terminates when the number of maximum iterative step $M = 30$ is reached or the infinity norm of the error between two adjacent iterative steps is less than 10^{-14} , i.e.,

$$\max_{1 \leq i \leq 2} \left\{ \|(k_i^1)^{l+1} - (k_i^1)^l\|_{\infty, h}, \|(k_i^2)^{l+1} - (k_i^2)^l\|_{\infty, h}, \|(k_i^3)^{l+1} - (k_i^3)^l\|_{\infty, h} \right\} < 10^{-14}.$$

5. Numerical results

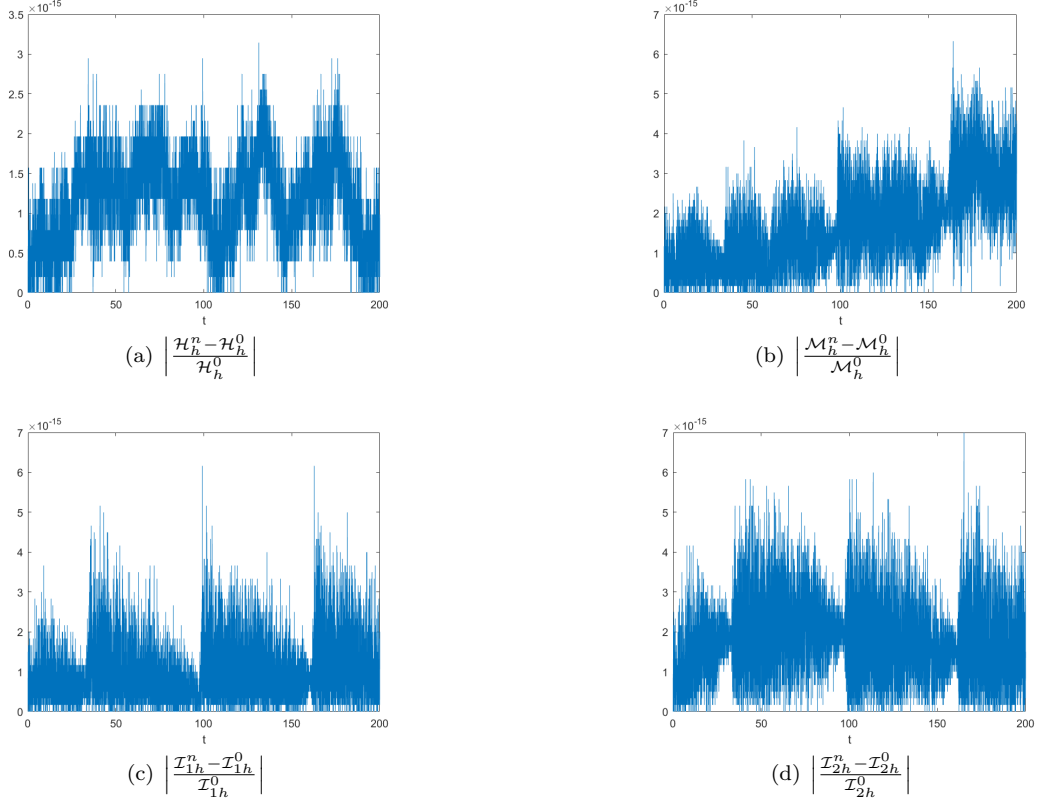


Figure 1: The errors of the discrete invariants of the FPRK-2 scheme for the ZR equation (1.1) with (5.2).

In this section, we will present some numerical examples of the ZR equation (1.1) to confirm the accuracy, stability, and conservation laws of the proposed numerical schemes. To testify the convergence rate, we denote

$$e_B = \|B(\cdot, t_n) - B^n\|_{h,\infty}, \quad e_\rho = \|\rho(\cdot, t_n) - \rho^n\|_{h,\infty}, \quad e_u = \|u(\cdot, t_n) - u^n\|_{h,\infty}.$$

5.1. Accuracy test

The ZR equation (1.1) admits a solitary-wave solution given by [24, 37]

$$\begin{aligned} B(x, t) &= \exp \left\{ i \left(\lambda t + \frac{c}{2\omega} (x - ct) + d_0 \right) \right\} R(x - ct + x_0), \\ \rho(x, t) &= -\frac{2c\kappa + \kappa\nu}{2\beta - 2(c + \nu)^2} |R(x - ct + x_0)|^2, \\ u(x, t) &= \frac{c\nu\kappa + \kappa\nu^2 - 2\kappa\beta}{2\beta - 2(c + \nu)^2} |R(x - ct + x_0)|^2, \end{aligned} \quad (5.1)$$

where

$$\lambda = \frac{4\omega^2\eta + c^2}{4\omega}, \quad \zeta = q + \frac{4c\nu\kappa + 3\kappa\nu^2 - 4\kappa\beta}{4\beta - 4(c + \nu)^2}, \quad R(x) = \sqrt{\frac{2\omega\eta}{\kappa\zeta}} \cdot \text{sech}(\sqrt{\eta}x),$$

and x_0 as well as d_0 represents the shifts of solitons in space and phase at $t = 0$, respectively. In this test, we choose computational domain $\Omega = [-32, 32]$, and set the parameters $\omega = \kappa = v = c = \eta = 1, \beta = 7, x_0 = 2$ and $d_0 = 0$. In view of the solitary-wave solution (5.1) with $t = 0$, the initial conditions are taken as

$$B_0(x) = B(x, 0), \quad \rho_0(x) = \rho(x, 0), \quad u_0(x) = u(x, 0), \quad x \in \Omega. \quad (5.2)$$

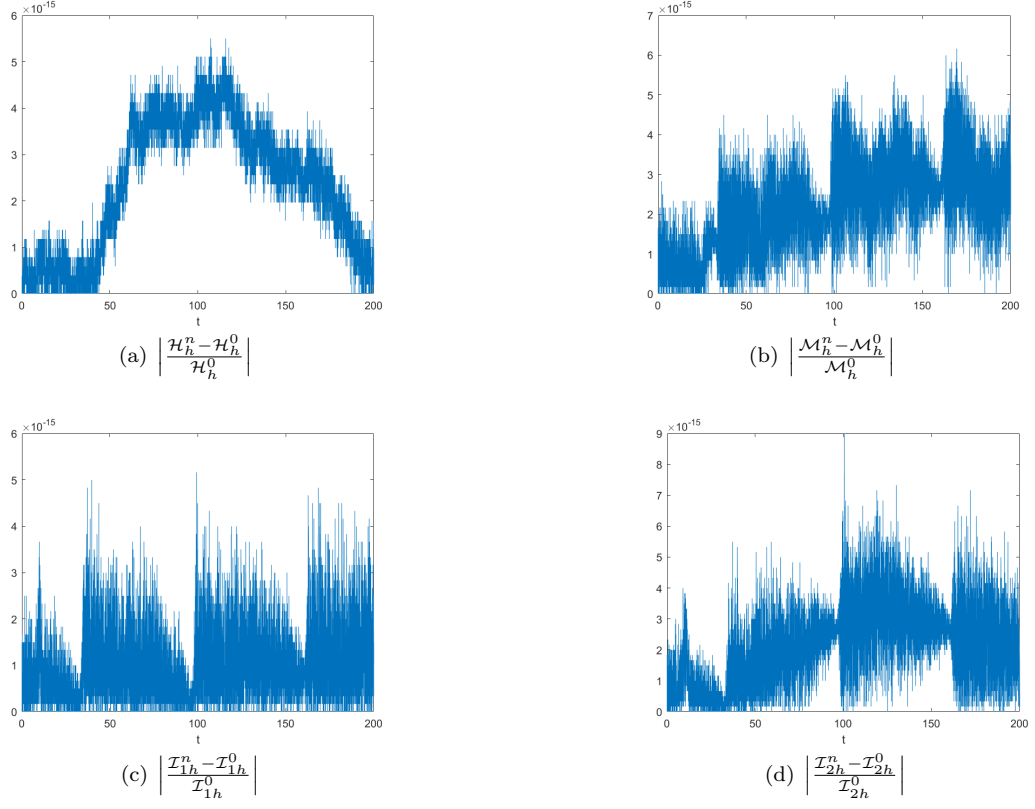


Figure 2: The errors of the discrete invariants of the FPRK-3 scheme for the ZR equation (1.1) with (5.2).

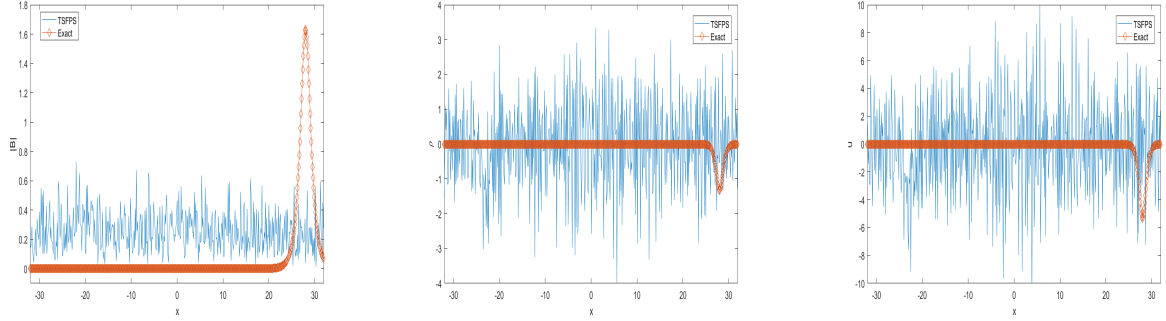


Figure 3: The numerical solution at $T = 30$ using the TS-FP scheme [37] for the ZR equation (1.1) with (5.2), $\tau = 1/20$ and $h = 1/8$.

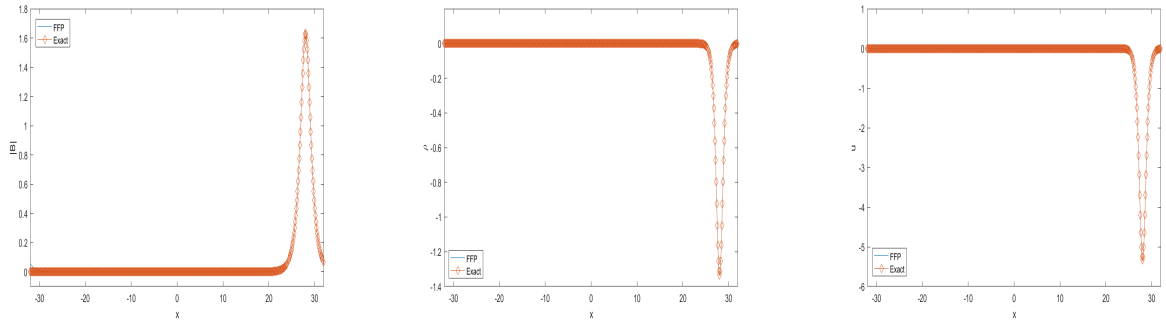


Figure 4: The numerical solution at $T = 30$ using the CN-FP scheme [38] for the ZR equation (1.1) with (5.2), $\tau = 1/20$ and $h = 1/8$.

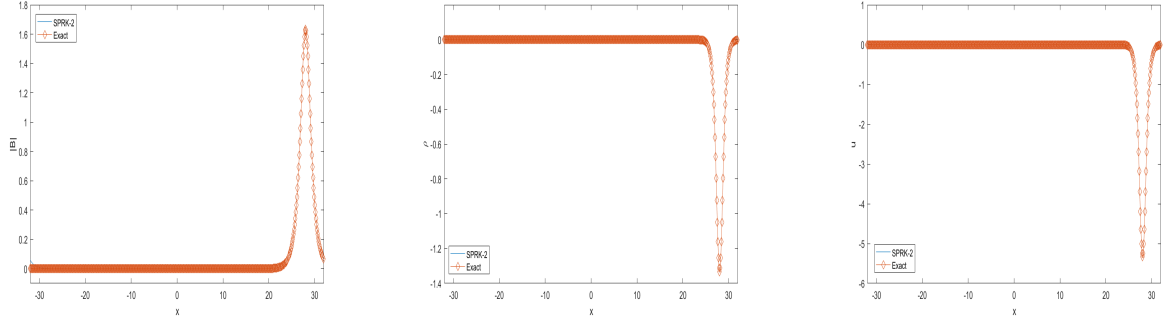


Figure 5: The numerical solution at $T = 30$ using the FPRK-2 scheme for the ZR equation (1.1) with (5.2), $\tau = 1/20$ and $h = 1/8$.

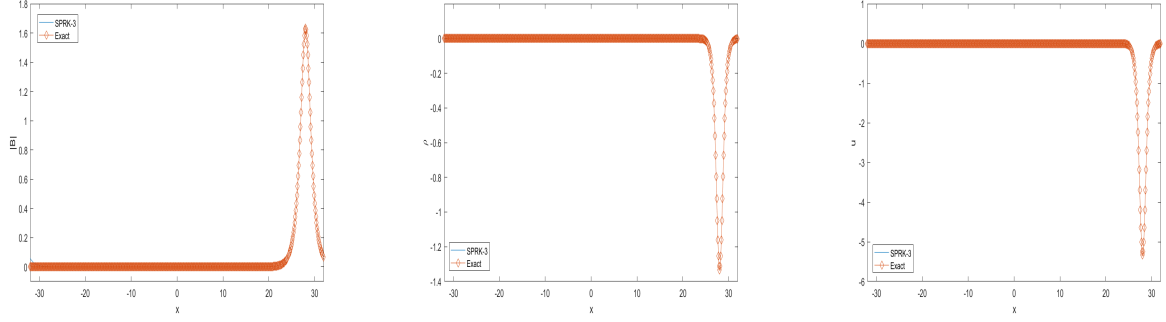


Figure 6: The numerical solution at $T = 30$ using the FPRK-3 scheme for the ZR equation (1.1) with (5.2), $\tau = 1/20$ and $h = 1/8$.

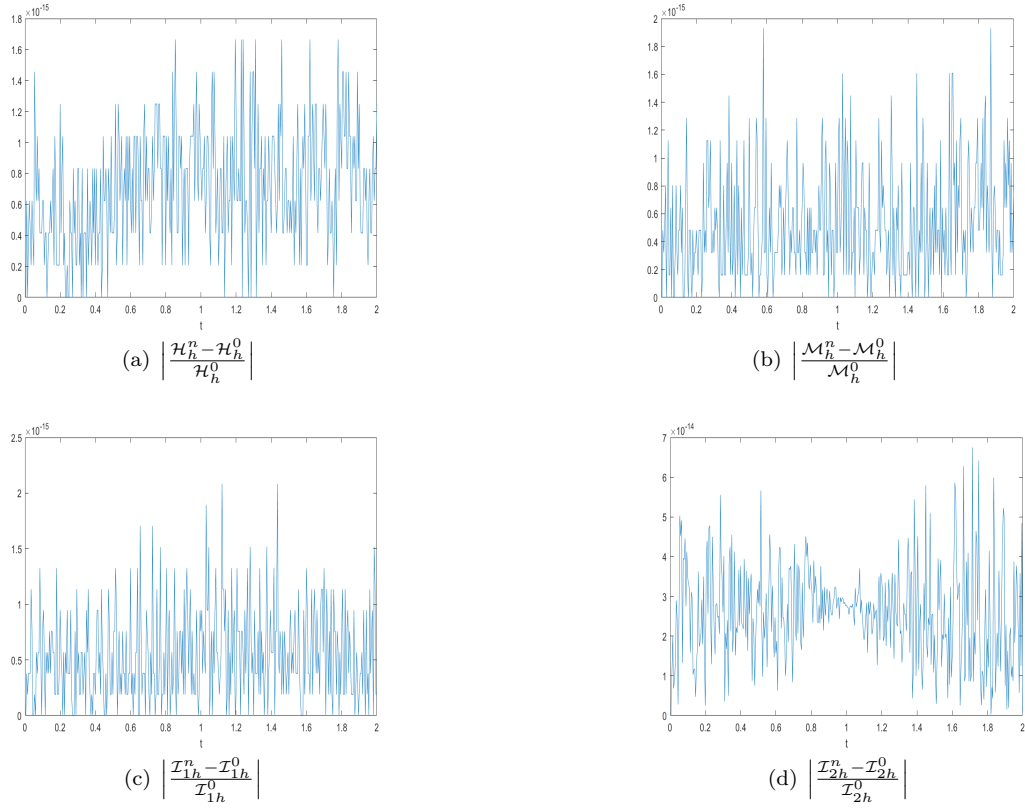


Figure 7: The errors of discrete invariants of the FPRK-2 scheme for the ZR equation (1.1) with (5.3) under case I.

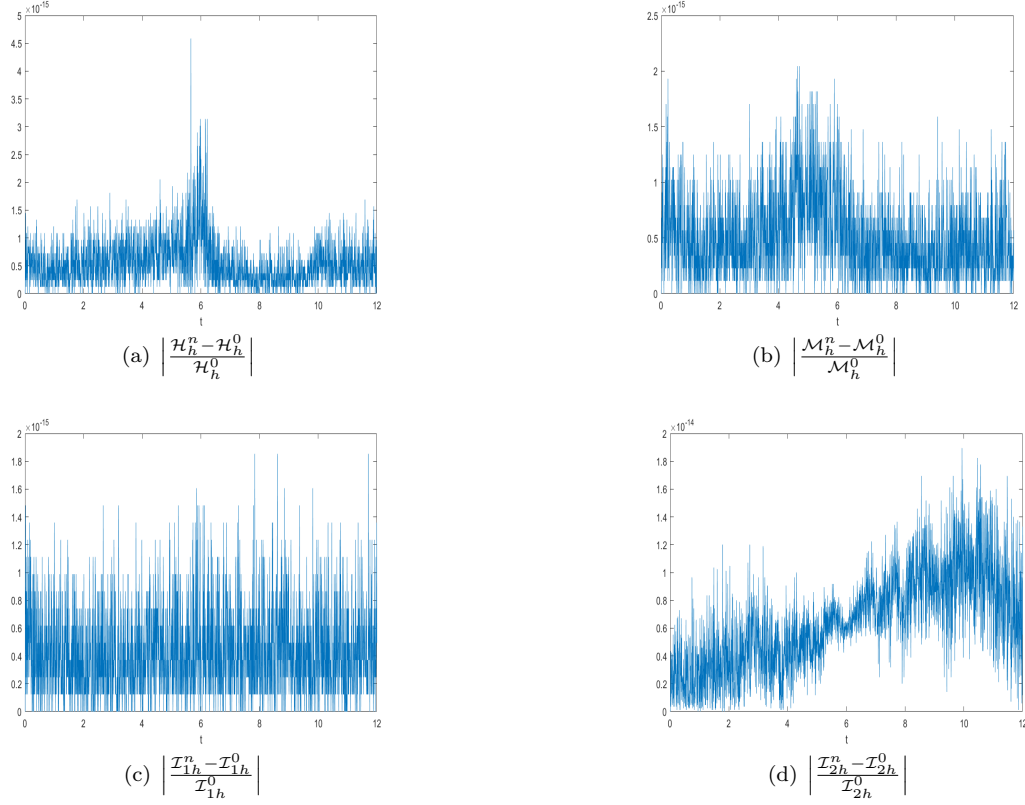


Figure 8: The errors of the discrete invariants of the FPRK-2 scheme for the ZR equation (1.1) with (5.3) under case II.

First, we test the spatial and temporal discretization error separately. Table 2 lists the spatial error of the FPRK- s schemes at $T = 4$ with a fixed time step size $\tau = 10^{-3}$ and different mesh size h . We observe that the spatial errors converge exponentially. Tables 3 and 4 list the temporal errors of the FPRK- s schemes with a fixed mesh size $h = 1/2^4$ and different time step size τ . It follows that the new methods are of fourth ($s = 2$) and sixth ($s = 3$) order accuracy in time. Next, Figures 1 and 2 display the conservation and the numerical errors with respect to time, respectively, where the computation was performed with $h = 1/2^4$, $\tau = 1/50$ until $T = 200$. We observe that the numerical scheme preserve the discrete mass and energy as well as other time invariants of the ZR equation (1.1) exactly.

Table 2: Spatial errors of the FPRK- s schemes at $T = 4$ for the ZR equation (1.1) with (5.2).

Scheme	Error	$h_0 = 1$	$h_0/2$	$h_0/2^2$	$h_0/2^3$
FPRK-2 scheme	e_B	5.97e-2	1.06e-4	1.42e-9	3.14e-13
	e_ρ	5.18e-2	7.34e-4	5.23e-8	1.13e-13
	e_u	1.16e-1	1.91e-3	1.24e-7	4.84e-13
FPRK-3 scheme	e_B	5.97e-2	1.06e-4	1.42e-9	3.14e-13
	e_ρ	5.18e-2	7.34e-4	5.23e-8	2.52e-14
	e_u	1.16e-1	1.91e-3	1.24e-07	8.08e-14

To verify the accuracy and efficiency, we investigated the maximum norm errors and computational time using the FPRK- s schemes, the TS-FP scheme [37] and the CN-FP scheme [38] at $T = 4$ under $\tau = 1/20$ and $h = 1/8$. The results are summarized in Table 5. These computational results illustrate that the errors of the FPRK- s schemes are much smaller at the same time steps, the TS-FP scheme and the CN-FP scheme converges at the second order in time. Subsequently, we also investigate the robustness of the FPRK- s scheme in simulating evolution of the soliton as a large time step $\tau = 1/20$, and the results are summarized in Figures 3-6. It is clear to see that (i) the computational results provided by the TS-FP scheme is wrong (Figure 3), although it is the most efficient; (ii) the energy-preserving schemes (the CN-FP scheme and the FPRK- s

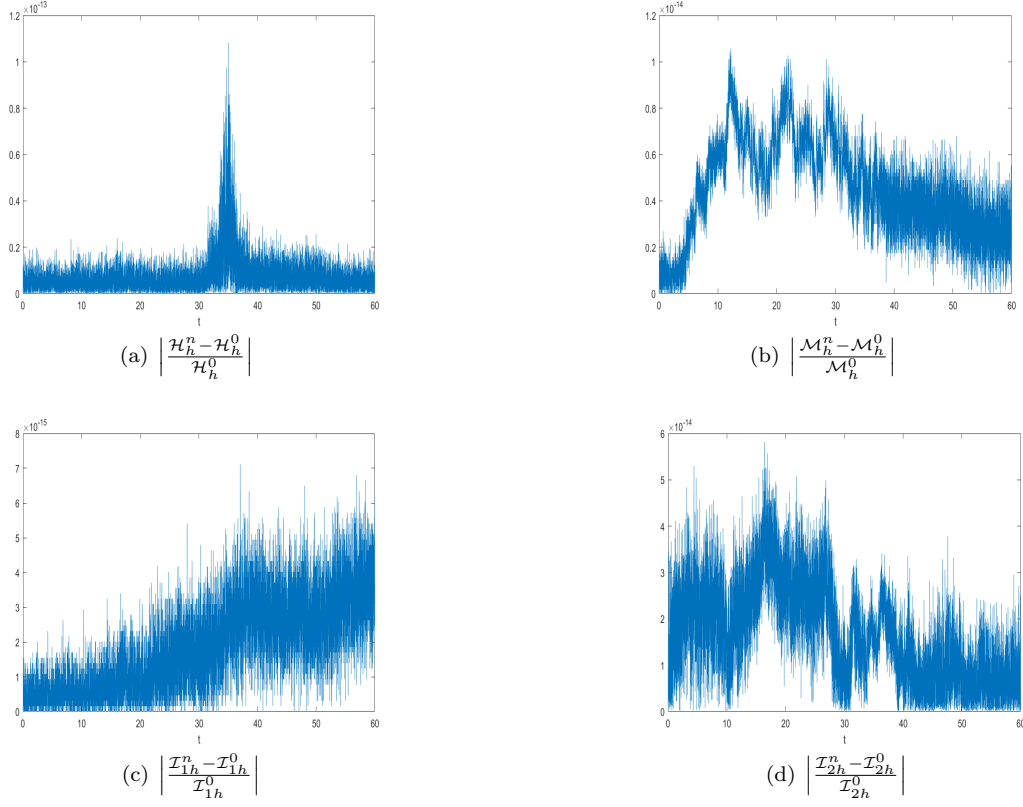


Figure 9: The errors of the discrete invariants of the FPRK-2 scheme for the ZR equation (1.1) with (5.3) under case III.

Table 3: Temporal errors of the FPRK-2 scheme at $T = 4$ for the ZR equation (1.1) with (5.2).

	$\tau_0 = 1/10$	$\tau_0/2$	$\tau_0/2^2$	$\tau_0/2^3$	$\tau_0/2^4$	$\tau_0/2^5$
e_B	1.05e-5	6.495e-7	4.04e-8	2.53e-9	1.58e-10	9.89e-12
rate	-	4.01	4.01	4.00	4.00	4.00
e_ρ	1.23e-5	7.87e-7	4.95e-8	3.10e-9	1.94e-10	1.21e-11
rate	-	3.97	3.99	4.00	4.00	4.00
e_u	4.56e-5	2.86e-6	1.79e-7	1.12e-8	7.01e-10	4.38e-11
rate	-	3.99	4.00	4.00	4.00	4.00

Table 4: Temporal errors of the FPRK-3 scheme at $T = 4$ for the ZR equation (1.1) with (5.2).

	$\tau_0 = 2/5$	$\tau_0/2$	$\tau_0/2^2$	$\tau_0/2^3$	$\tau_0/2^4$	$\tau_0/2^5$
e_B	7.10e-5	2.46e-6	2.60e-8	3.32e-10	5.35e-12	3.15e-13
rate	-	4.85	6.56	6.29	5.95	4.09
e_ρ	1.53e-4	3.09e-6	4.48e-8	6.37e-10	9.76e-12	1.32e-13
rate	-	5.63	6.11	6.14	6.03	6.21
e_u	4.04e-4	5.60e-6	5.93e-8	9.40e-10	1.47e-11	2.66e-13
rate	-	6.17	6.56	5.98	5.99	5.79

schemes) simulate the soliton well (Figures 4-6).

Table 5: Comparison of numerical errors and computational time for the ZR (1.1) with (5.2).

Scheme	Error	$\tau_0 = 1/5$	$\tau_0/2$	$\tau_0/2^2$	$\tau_0/2^3$	$\tau_0/2^4$
TS-FP scheme	e_B	6.03e-1	5.78e-2	1.52e-2	3.65e-3	9.14e-4
	e_ρ	8.75e-1	4.90e-2	1.31e-2	2.75e-3	6.94e-4
	e_u	1.94e+0	1.90e-1	4.88e-2	1.14e-2	2.85e-3
	time(s)	0.01	0.01	0.02	0.05	0.09
CN-FP scheme	e_B	5.22e-2	1.29e-2	3.22e-3	8.04e-4	2.01e-4
	e_ρ	4.07e-2	8.58e-3	2.12e-3	5.28e-4	1.32e-4
	e_u	1.41e-1	3.04e-2	7.52e-3	1.87e-3	4.68e-4
	time(s)	0.13	0.15	0.22	0.33	0.57
FPRK-2 scheme	e_B	1.74e-4	1.05e-5	6.48e-7	4.04e-8	2.52e-9
	e_ρ	1.91e-4	1.23e-5	7.79e-7	4.87e-8	3.05e-9
	e_u	7.09e-4	4.42e-5	2.78e-6	1.74e-7	1.09e-8
	time(s)	0.19	0.27	0.44	0.77	1.13
FPRK-3 scheme	e_B	2.46e-6	2.60e-8	3.32e-10	5.35e-12	3.15e-13
	e_ρ	3.09e-6	4.48e-8	6.37e-10	9.76e-12	1.32e-13
	e_u	5.60e-6	5.93e-8	9.40e-10	1.47e-11	2.66e-13
	time(s)	0.66	0.84	1.85	2.13	3.22

5.2. Interactions of solitons

The initial data are then selected as (cf. [37])

$$\begin{aligned}
B_0(x) &= \exp \left\{ i \left(\frac{c_+}{2\omega} x + d_0 \right) \right\} R_+(x + x_{0+}) + \exp \left\{ i \left(\frac{c_-}{2\omega} x + d_0 \right) \right\} R_-(x + x_{0-}), \\
\rho_0(x) &= -\frac{2c_+\kappa + \kappa\nu}{2\beta - 2(c_+ + \nu)^2} |R_+(x + x_{0+})|^2 - \frac{2c_-\kappa + \kappa\nu}{2\beta - 2(c_- + \nu)^2} |R_-(x + x_{0-})|^2, \\
u_0(x) &= \frac{c_+\nu\kappa + \kappa\nu^2 - 2\kappa\beta}{2\beta - 2(c_+ + \nu)^2} |R_+(x + x_{0+})|^2 + \frac{c_-\nu\kappa + \kappa\nu^2 - 2\kappa\beta}{2\beta - 2(c_- + \nu)^2} |R_-(x + x_{0-})|^2, \quad x \in [a, b],
\end{aligned} \tag{5.3}$$

where c_\pm and $x_{0\pm}$ are different velocities and different initial locations of the two solitary waves, respectively, $\eta_\pm > 0$, and

$$\lambda_\pm = \frac{4\omega^2\eta_\pm + c_\pm^2}{4\omega}, \quad \zeta_\pm = q + \frac{4c_\pm\nu\kappa + 3\kappa\nu^2 - 4\kappa\beta}{4\beta - 4(c_\pm + \nu)^2}, \quad R_\pm(x) = \sqrt{\frac{2\omega\eta_\pm}{\kappa\zeta_\pm}} \cdot \operatorname{sech}(\sqrt{\eta_\pm}x).$$

All numerical calculations are performed by using the numerical schemes with $h = 1/8$, $\tau = 1/200$, and the parameters are taken as:

Case I: High velocity case:

$$\begin{aligned}
\omega &= \eta_\pm = 1, \quad \kappa = 2, \quad \nu = 0.2, \quad c_\pm = \pm 8, \quad x_{0\pm} = \pm 8, \quad \beta = 75, \quad d_0 = 0, \\
-a &= b = 20, \quad T = 2;
\end{aligned}$$

Case II: Intermediate velocity case:

$$\begin{aligned}
\omega &= \eta_\pm = 1, \quad \kappa = 3, \quad \nu = 0.2, \quad c_\pm = \pm 1.5, \quad x_{0\pm} = \pm 9, \quad \beta = 12, \quad d_0 = 0, \\
-a &= b = 24, \quad T = 12;
\end{aligned}$$

Case III: Small velocity case:

$$\begin{aligned}
\omega &= \eta_\pm = 1, \quad \kappa = 1, \quad \nu = 0.5, \quad c_+ = 0, \quad c_- = -0.5, \quad x_{0+} = -8, \quad x_{0-} = -26, \\
\beta &= 3, \quad d_0 = 0, \quad -a = b = 70, \quad T = 60.
\end{aligned}$$

The simulation of the surface plots and contour plots of collisions for $|B(x, t)|$, $\rho(x, t)$ and $u(x, t)$ under cases I-III are drawn in Figures 10-12, respectively. We can observe that all the collisions between two solitons

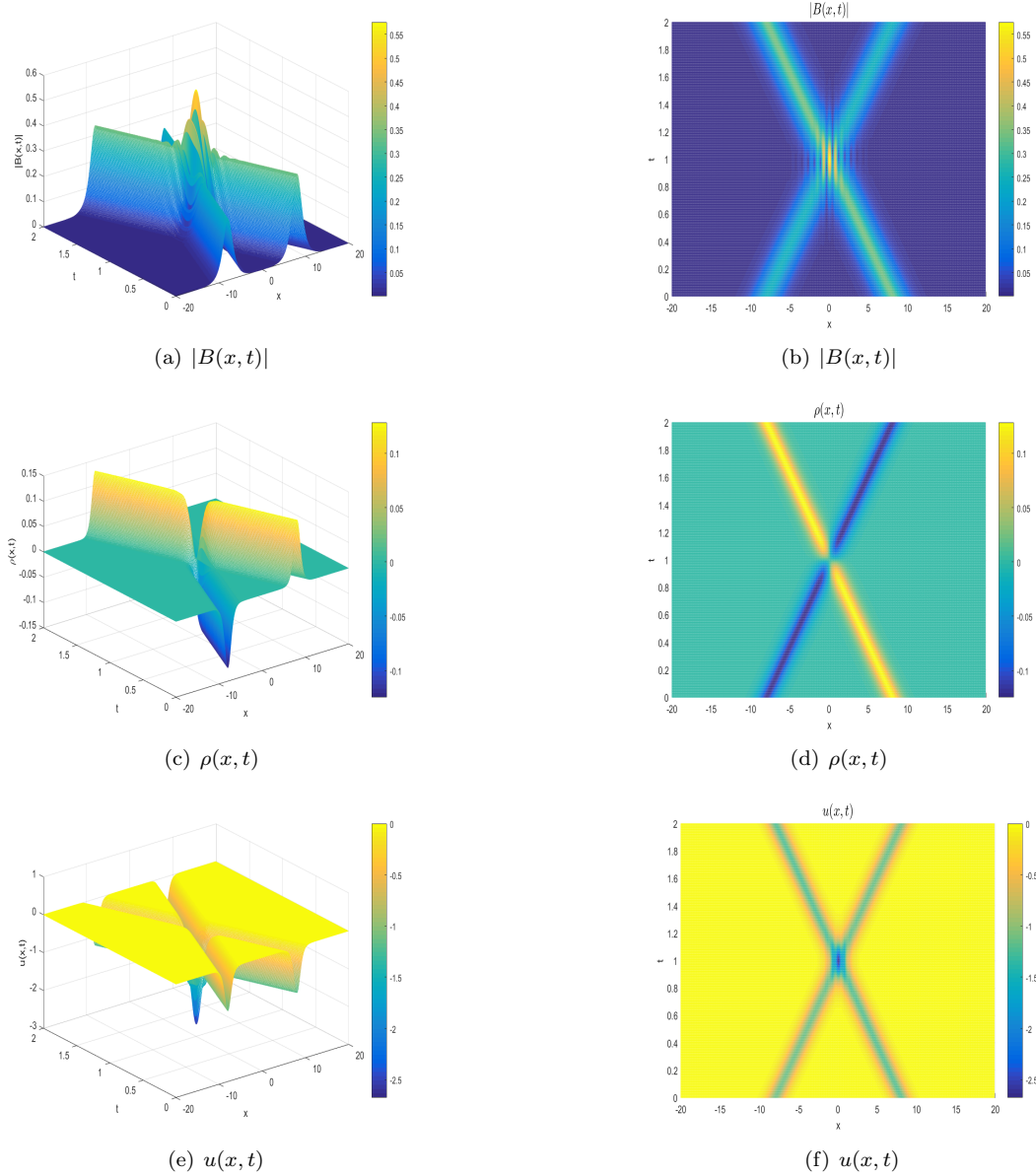


Figure 10: Inelastic collision between two solitons of the FPRK-2 scheme for the ZR equation (1.1) with (5.3) under case I.

are not elastic. From Figures 11-12, one can see, some little dispersive waves are produced throughout the collision or following the collision. This means, the ZR equation (1.1) is a non-integrable system [37, 25, 38]. The obtained outcomes in this subsection are completely in good agreement with those presented in literatures [37, 25, 38].

To demonstrate the advantages of the proposed high-order FPRK- s schemes with the non-energy-preserving scheme, we summarized the evolution of numerical simulation of soliton collisions using the large time step $\tau = 1/20$ and $h = 1/8$ under case (III) in Figures 12-14. It is observed that the FPRK-2 scheme (Figure 12) and the CN-FPS scheme (Figure 13) have a good numerical performance on long time simulations even in the cases of very rough discretizations, while the TS-FP scheme (Figure 14) is failed to represent the solution accurately. This agrees totally with the analytical results established in [29, 35].

6. Conclusion

In this paper, we propose a novel high-order energy-preserving scheme extending the classical Crank-Nicolson proposed method in [37, 38] to high order. Based on the idea of the QAV approach, we first transform

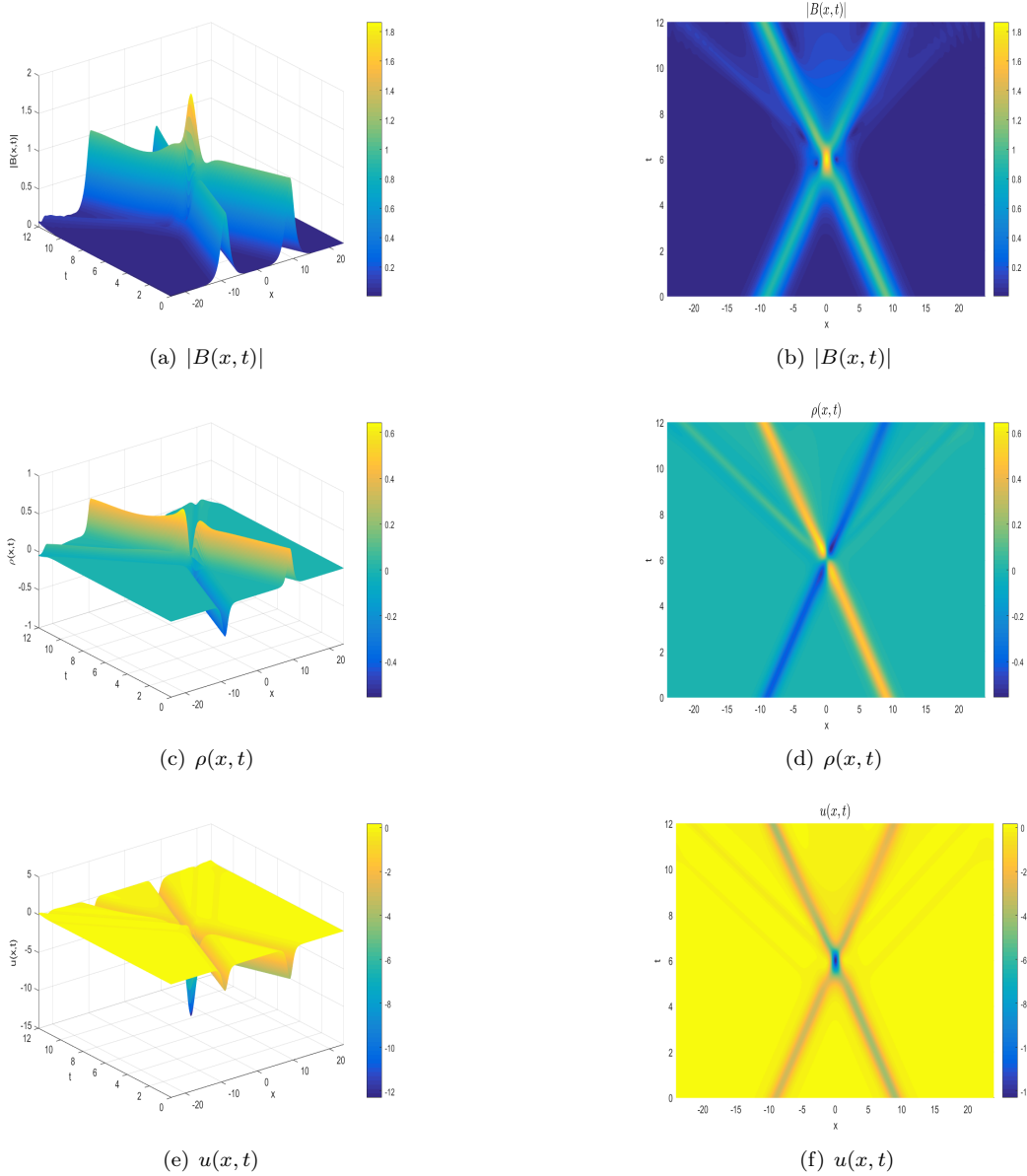


Figure 11: Inelastic collision between two solitons of the FPRK-2 scheme for the ZR equation (1.1) with (5.3) under case II.

the Hamiltonian energy into a quadratic form by introducing a quadratic auxiliary variable, and the original system is then reformulated into a new equivalent system using the energy variational principle. Finally, a fully-discrete scheme is presented by using the symplectic RK method in time and the Fourier pseudo-spectral method in space for the reformulated system. We show that the proposed scheme can preserve the three invariants (1.4)-(1.5) of the ZR equation (1.1) exactly. In addition, an efficient iterative solver is presented to solve the discrete nonlinear equations of our scheme. Numerical results show that the proposed scheme has more advantages than the TS-FP scheme [37] in the robustness and the long-time accurate computations. However, we should note that the proposed scheme is fully-implicit. Thus, an interesting topic for future studies is whether it is possible to construct high-order linearly implicit schemes which can preserve the three invariants (1.4)-(1.5) of the ZR equation (1.1) exactly.

Acknowledgment

The work is supported by the National Natural Science Foundation of China (Grant Nos.11701110, 11901513), and the Yunnan Fundamental Research Projects (Grant Nos. 202101AT070208, 202101AS070044),

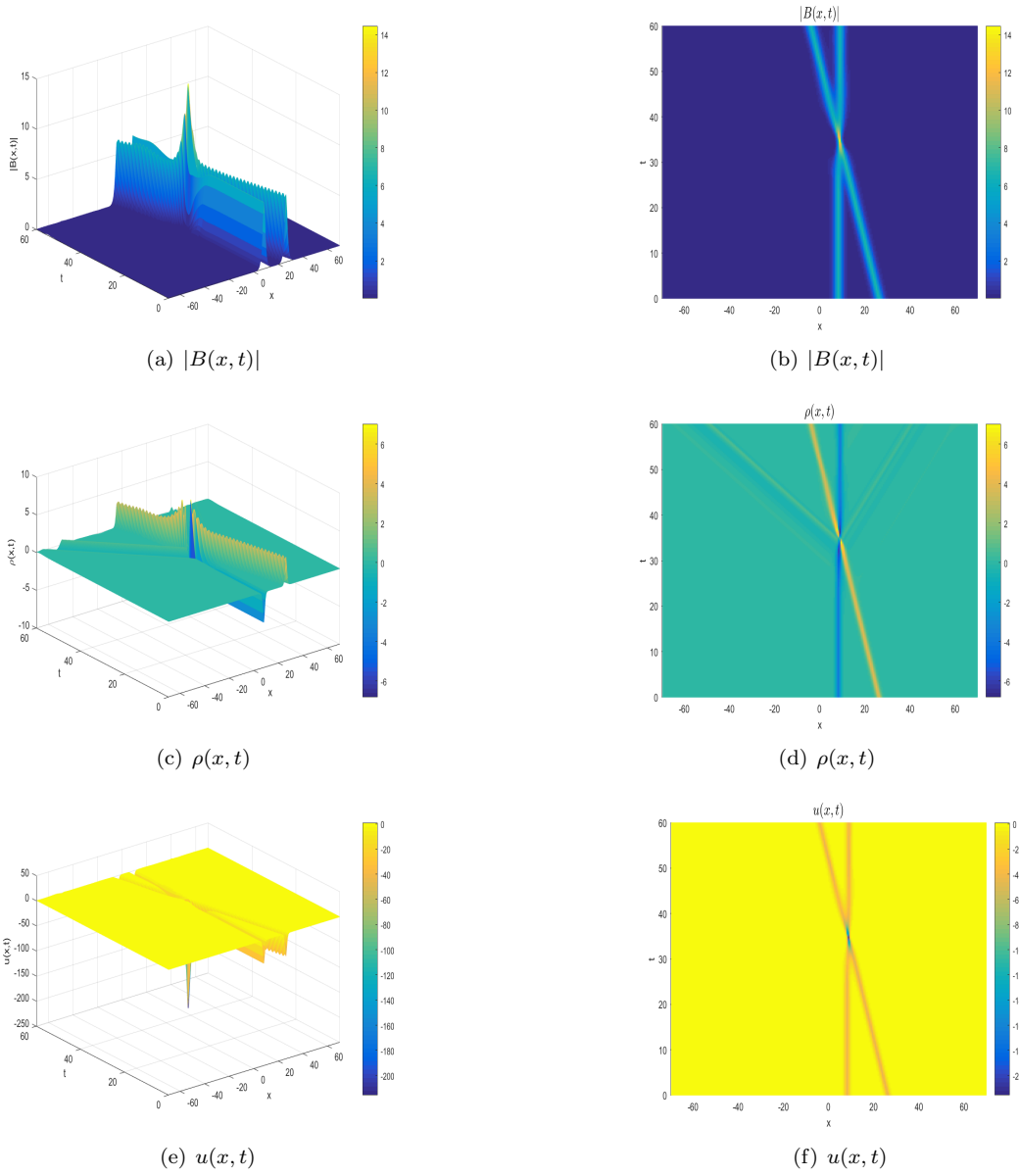


Figure 12: Inelastic collision between two solitons of the FPRK-2 scheme for the ZR equation (1.1) with (5.3) under case III.

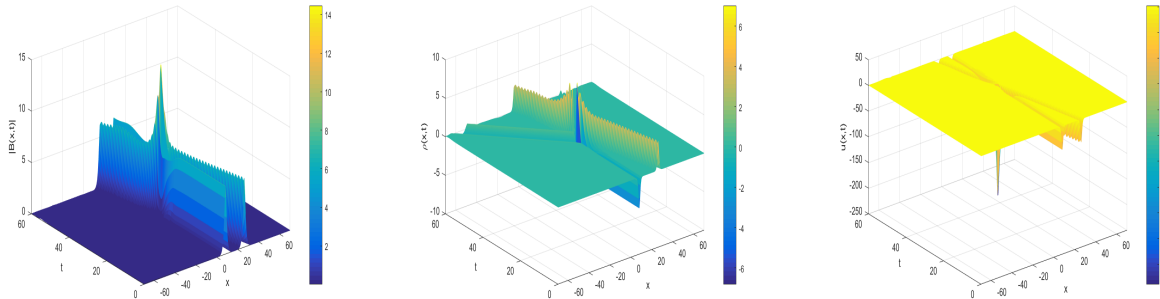


Figure 13: Inelastic collision between two solitons of the CN-FP scheme [38] for the ZR equation (1.1) with (5.3) under cases (III).

and the Natural Science Foundation of Hunan (Grant No. 2021JJ40655). The first author is in particular grateful to Prof. Weizhu Bao for fruitful discussions.

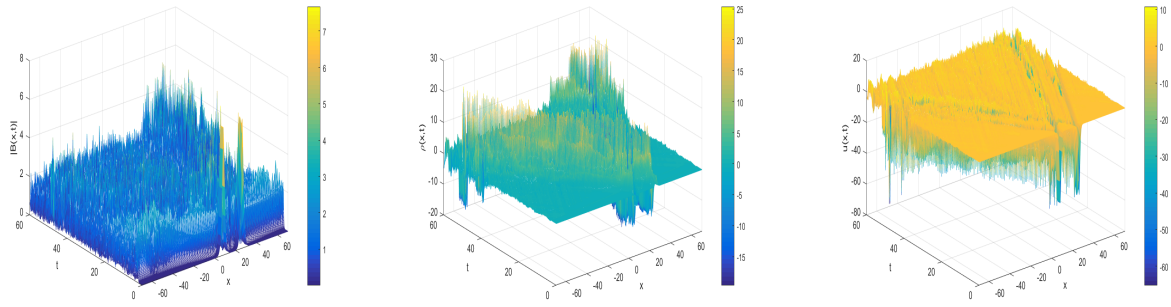


Figure 14: Inelastic collision between two solitons of the TS-FP scheme [37] for the ZR equation (1.1) with (5.3) under cases (III).

References

- [1] L. Barletti, L. Brugnano, G. F. Caccia, and F. Iavernaro. Energy-conserving methods for the nonlinear Schrödinger equation. *Appl. Math. Comput.*, 318:3–18, 2018.
- [2] L. Brugnano and F. Iavernaro. *Line Integral Methods for Conservative Problems*. Chapman et Hall/CRC: Boca Raton, FL, USA, 2016.
- [3] L. Brugnano, F. Iavernaro, and D. Trigiante. Hamiltonian boundary value methods (energy preserving discrete line integral methods). *J. Numer. Anal. Ind. Appl. Math.*, 5:17–37, 2010.
- [4] M. Calvo, A. Iserles, and A. Zanna. Numerical solution of isospectral flows. *Math. Comp.*, 66:1461–1486, 1997.
- [5] J. Chen and M. Qin. Multi-symplectic Fourier pseudospectral method for the nonlinear Schrödinger equation. *Electr. Trans. Numer. Anal.*, 12:193–204, 2001.
- [6] D. Cohen and E. Hairer. Linear energy-preserving integrators for Poisson systems. *BIT*, 51:91–101, 2011.
- [7] G. J. Cooper. Stability of Runge-Kutta methods for trajectory problems. *IMA J. Numer. Anal.*, 7:1–13, 1987.
- [8] J. Cordero. Supersonic limit for the Zakharov–Rubenchik system. *J. Differ. Equ.*, 261:5260–5288, 2016.
- [9] J. Cui, Y. Wang, and C. Jiang. Arbitrarily high-order structure-preserving schemes for the Gross-Pitaevskii equation with angular momentum rotation. *Comput. Phys. Commun.*, 261:107767, 2021.
- [10] Y. Gong, Y. Chen, C. Wang, and Q. Hong. A new class of high-order energy-preserving schemes for the Korteweg-de Vries equation based on the quadratic auxiliary variable (QAV) approach. *arXiv: 2108.12097v1*, 2021.
- [11] E. Hairer. Energy-preserving variant of collocation methods. *J. Numer. Anal. Ind. Appl. Math.*, 5:73–84, 2010.
- [12] E. Hairer, C. Lubich, and G. Wanner. *Geometric Numerical Integration: Structure-Preserving Algorithms for Ordinary Differential Equations*. Springer-Verlag, Berlin, 2nd edition, 2006.
- [13] B. Ji, L. Zhang, and X. Zhou. Conservative compact difference scheme for the Zakharov–Rubenchik equations. *Int. J. Comput. Math.*, 96:537–556, 2019.
- [14] C. Jiang, J. Cui, X. Qian, and S. Song. High-order linearly implicit structure-preserving exponential integrators for the nonlinear Schrödinger equation. *J. Sci. Comput.*, 90:66, 2022.
- [15] C. Jiang, Y. Wang, and Y. Gong. Arbitrarily high-order energy-preserving schemes for the Camassa-Holm equation. *Appl. Numer. Math.*, 151:85–97, 2020.
- [16] H. Li, Y. Wang, and M. Qin. A sixth order averaged vector field method. *J. Comput. Math.*, 34:479–498, 2016.

- [17] Y. Li and X. Wu. General local energy-preserving integrators for solving multi-symplectic Hamiltonian PDEs. *J. Comput. Phys.*, 301:141–166, 2015.
- [18] Y. Li and X. Wu. Functionally fitted energy-preserving methods for solving oscillatory nonlinear Hamiltonian systems. *SIAM J. Numer. Anal.*, 54:2036–2059, 2016.
- [19] F. Linares and C. Matheus. Well-posedness for the 1D Zakharov–Rubenchik system. *Adv. Differ. Eq.*, 14:261–288, 2009.
- [20] L. Mei, L. Huang, and X. Wu. Energy-preserving exponential integrators of arbitrarily high order for conservative or dissipative systems with highly oscillatory solutions. *J. Comput. Phys.*, 442:110429, 2021.
- [21] Y. Miyatake and J. C. Butcher. A characterization of energy-preserving methods and the construction of parallel integrators for Hamiltonian systems. *SIAM J. Numer. Anal.*, 54:1993–2013, 2016.
- [22] F. Oliveira. Stability of the solitons for the one-dimensional Zakharov–Rubenchik equation. *Phys. D.*, 175:220–240, 2003.
- [23] F. Oliveira. Adiabatic limit of the Zakharov–Rubenchik equation. *Rep. Math. Phys.*, 61:13–27, 2008.
- [24] F. Oliveira. Stability of solutions of the Zakharov–Rubenchik equation. *Wave Sta. Contin. Media*, pages 408–413, 2015.
- [25] Ö. Oruç. A radial basis function finite difference (RBF–FD) method for numerical simulation of interaction of high and low frequency waves: Zakharov–Rubenchik equations. *Appl. Math. Comput.*, 394:125787, 2021.
- [26] G. Ponce and J. C. Saut. Well-posedness for the Benney–Roskes/Zakharov–Rubenchik system. *Discret. Contin. Dyn. Syst.*, 13:818–852, 2005.
- [27] G. R. W. Quispel and D. I. McLaren. A new class of energy-preserving numerical integration methods. *J. Phys. A: Math. Theor.*, 41:045206, 2008.
- [28] J. M. Sanz-Serna. Runge-Kutta schemes for Hamiltonian systems. *BIT*, 28:877–883, 1988.
- [29] J. M. Sanz-Serna and J. G. Verwer. Conservative and nonconservative schemes for the solution of the nonlinear Schrödinger equation. *IMA J. Numer. Anal.*, 6:25–42, 1986.
- [30] J. Shen and T. Tang. *Spectral and High-Order Methods with Applications*. Science Press, Beijing, 2006.
- [31] W. Tang and Y. Sun. Time finite element methods: a unified framework for numerical discretizations of ODEs. *Appl. Math. Comput.*, 219:2158–2179, 2012.
- [32] B. K. Tapley. Numerical integration of ODEs while preserving all polynomial first integrals. *arXiv preprint arXiv:2108.06548*, 2021.
- [33] B. Wang and Y. Jiang. Optimal convergence and long-time conservation of exponential integration for schrödinger equations in a normal or highly oscillatory regime. *J. Sci. Comput.*, 90:1–31, 2022.
- [34] V. E. Zakharov and A. M. Rubenchik. Nonlinear interaction between high and low frequency waves. *Prikl. Mat. Techn. Fiz.*, 5:84–89, 1972.
- [35] F. Zhang, V. M. Pérez-García, and L. Vázquez. Numerical simulation of nonlinear Schrödinger systems: a new conservative scheme. *Appl. Math. Comput.*, 71:165–177, 1995.
- [36] G. Zhang and C. Jiang. Arbitrary high-order structure-preserving methods for the quantum Zakharov system. *arXiv:2202.13052*, 2022.
- [37] X. Zhao and Z. Li. Numerical methods and simulations for the dynamics of one-dimensional Zakharov–Rubenchik equations. *J. Sci. Comput.*, 59:412–438, 2014.
- [38] X. Zhou, T. Wang, and L. Zhang. Two numerical methods for the Zakharov–Rubenchik equations. *Adv. Comput. Math.*, 45:1163–1184, 2019.